Time will tell: temporal evolution of Martian gullies and paleoclimatic implications

T. de Haas[1,2], S. J. Conway[3], F. E. G. Butcher[4], J. Levy[5], P. M. Grindrod[6,7], T. A. Goudge[5], M. R. Balme[4]

[1]Faculty of Geosciences, Universiteit Utrecht, Utrecht, The Netherlands.

[2]Department of Geography, Durham University, Durham, UK.

[3]Laboratoire de Planétologie et Géodynamique, Université de Nantes, Nantes, France.

[4]School of Physical Sciences, The Open University, Milton Keynes, UK.

[5]Jackson School of Geosciences, University of Texas, Austin, USA.

[6]Department of Earth and Planetary Sciences, Birkbeck, University of London, London, UK.

[7]Centre for Planetary Sciences, UCL/Birkbeck, London, UK.

Corresponding author: T. de Haas, t.dehaas@uu.nl

Abstract

To understand Martian paleoclimatic conditions and the role of volatiles therein, the spatio-temporal evolution of gullies must be deciphered. While the spatial distribution of gullies has been extensively studied, their temporal evolution is poorly understood. We show that gully-size is similar in very young and old craters. Gullies on the walls of very young impact craters ($<$ a few Myr) typically cut into bedrock and are free of latitude-dependent mantle (LDM) and glacial deposits, while such deposits become increasingly evident in older craters. These observations suggest that gullies go through obliquity-driven degradation/accumulation cycles over time controlled by (1) LDM emplacement and degradation and by (2) glacial emplacement and removal. In glacially-influenced craters the distribution of gullies on crater walls coincides with the extent of glacial deposits, which suggests that melting of snow and ice played a role in the formation of these gullies. Yet, present-day activity is observed in some gullies on formerly glaciated crater walls. Moreover, in very young craters extensive gullies have formed in the absence of LDM and glacial deposits, showing that gully formation can also be unrelated to these deposits. The Martian climate varied substantially over time, and the gully-forming mechanisms likely varied accordingly.

1 Introduction

Martian gullies are landforms that consist of an alcove, channel and depositional apron [e.g., *Malin and Edgett*, 2000]. Reconstructing the conditions and processes under which these gullies have formed is key to understanding past climatic conditions on Mars. The formation of gullies has been attributed to (1) water-free sediment flows, either without a volatile [e.g., *Treiman*, 2003; *Pelletier et al.*, 2008] or triggered by sublimation of CO_2 frost [e.g., *Cedillo-Flores et al.*, 2011; *Dundas et al.*, 2012, 2015; *Pilorget and Forget*, 2016] and (2) aqueous debris flows [e.g., *Costard et al.*, 2002; *Levy et al.*, 2010a; *Conway et al.*, 2011; *Johnsson et al.*, 2014; *De Haas et al.*, 2015a,b] and fluvial flows (hyperconcentrated or dilute) [e.g., *Heldmann and Mellon*, 2004; *Heldmann et al.*, 2005; *Dickson et al.*, 2007; *Head et al.*, 2008; *Reiss et al.*, 2011]. Each of these formation processes has different implications for Mars' current and recent water-cycle, therefore the presence of habitable environments and resources for future exploration. To better understand the Martian paleoclimate and the role of volatiles therein the spatio-temporal evolution of gullies needs to be understood in detail. While the spatial distribution of gullies has been extensively studied and quantified [e.g., *Heldmann and Mellon*, 2004; *Balme et al.*, 2006; *Dickson et al.*, 2007; *Kneissl et al.*, 2010; *Harrison et al.*, 2015], only few studies have addressed their temporal evolution [e.g., *Dickson et al.*, 2015; *De Haas et al.*, 2015b]. When studied, the temporal evolution of gullies has mainly been performed on the basis of local and/or qualitative assessments [*Head et al.*, 2008; *Schon et al.*, 2009; *Raack et al.*, 2012]. Yet, for a more detailed temporal understanding quantitative analyses of age constraints and gully size, morphology and morphometry on a global scale are crucial [*Conway and Balme*, 2014, 2016; *De Haas et al.*, 2015c].

Gullies occur in the mid- and high latitudes of Mars, from the poles down to 30° latitudes in the northern and southern hemisphere [e.g., *Heldmann and Mellon*, 2004; *Balme et al.*, 2006; *Dickson et al.*, 2007; *Kneissl et al.*, 2010; *Harrison et al.*, 2015]. The global distribution of gullies corresponds well with the distribution of surface features indicative of past and/or present near-surface ground ice and glacial activity, such as lobate debris aprons (LDA) [*Squyres*, 1979], viscous flow features [*Milliken et al.*, 2003] and the latitude dependent mantle (LDM; a smooth, often meters-thick deposit thought to consist of ice with a minor component of dust) [e.g., *Head et al.*, 2003]. Gullies are predominantly poleward-facing in the lower midlatitudes, shift to mainly equator-facing at $\sim$45° latitude at both hemispheres and no preferential gully-orientation is found near the poles [*Balme et al.*, 2006; *Kneissl et al.*, 2010; *Harrison et al.*, 2015;

Conway, This Issue]. These observations point towards insolation and atmospheric conditions playing key roles in the formation of Martian gullies.

Some authors suggest that gullies predominantly form during glacial periods forced by high orbital obliquity [e.g., *Head et al.*, 2003, 2008; *Dickson and Head*, 2009; *Dickson et al.*, 2015], whilst observation of gullies that are morphologically active today have led other authors to suggest that gully-formation may have been unrelated to these climatic cycles [e.g., *Dundas et al.*, 2010, 2015]. Gullies are typically recognized as geologically very young features, owing to a conspicuous absence of superposed impact craters [e.g., *Malin and Edgett*, 2000], superposition relationships with polygons, dunes and transverse aeolian ridges [e.g., *Malin and Edgett*, 2000; *Reiss et al.*, 2004], and their occurrence in young impact craters that formed within the last few million years [*Schon et al.*, 2009; *Johnsson et al.*, 2014; *De Haas et al.*, 2015c]. *De Haas et al.* [2015c] noted that the size of gullies in relatively pristine host craters is typically similar to the size of gullies found in much older host craters, implying the presence of processes limiting gully growth over time. Gully growth may be limited by: (a) decreasing geomorphological activity in gullies over time following crater formation [*De Haas et al.*, 2015c], (b) the latitude-dependent mantle acting as a barrier to bedrock-incision and enlargement once established [*De Haas et al.*, 2015c], (c) alternating erosional/depositional episodes driven by orbital cycles [*Dickson et al.*, 2015] or (d) a combination of these factors. Additionally, we know that some gully-fans are fed by alcoves that cut into bedrock [e.g., *Johnsson et al.*, 2014; *De Haas et al.*, 2015c; *Núñez et al.*, 2016] while other gully-fans are fed by alcoves cutting into LDM or glacial deposits [e.g., *Head et al.*, 2008; *Conway and Balme*, 2014; *Núñez et al.*, 2016], which may be related to the evolution of the host-crater wall over time. The exact temporal evolution and associated formative mechanisms of gullies, however, remain to be determined.

Here we aim to quantitatively constrain the temporal evolution of Martian gullies. More specifically, we aim to (1) investigate how time and associated climatic variations have affected gullies, (2) provide a conceptual model for the temporal evolution of gullies and (3) deduce paleoclimatic and paleohydrologic conditions from the inferred temporal evolution of gullies.

This paper is organized as follows. We first detail study sites, materials and methods. Then we describe the morphology of the gullies and associated landforms in the studied craters, determine gully-size and host crater age, and infer trends of gully morphology and size versus host crater age. Subsequently, we present a conceptual model for the temporal evolution

of gullies. Thereafter, we place the relation between gully morphology and associated landforms and host crater age in an obliquity framework. Next, we draw paleoclimatic implications based on the results presented here. We end with a brief discussion on the potential spatial variations on the temporal trends inferred in this paper.

2 Materials and methods

We compare the size of gullies in 19 craters, of which 17 are spread over the southern midlatitudes and 2 occur in the northern midlatitudes (Fig. 1, Table 1). These study sites were selected based on the following criteria: (1) the presence of gullies, (2) the presence of a high-resolution digital terrain model (DTM) made from High Resolution Science Imaging Experiment (HiRISE) [*McEwen et al.*, 2007] stereo images ($\sim$1 m spatial resolution) or the presence of suitable stereo images to produce a DTM ourselves, and (3) a well-defined ejecta blanket that has not undergone major resurfacing events since emplacement. The latter enables dating of the ejecta blanket of the crater hosting the gullies, and thereby constraining the earliest possible start point and thus the maximum duration of gully activity.

The dataset comprises all publicly available HiRISE DTMs showing gullies for which dating of the host crater was possible (as of 1 March 2016). Moreover, additional HiRISE DTMs that were previously made by the authors were added to the dataset (Table 2). These DTMs were produced with the software packages ISIS3 and SocetSet following the workflow described by *Kirk et al.* [cf. 2008] (DTM credit Open University or Birkbeck University of London in Table 2) or with the Ames Stereo Pipeline [cf. *Broxton and Edwards*, 2008; *Beyer et al.*, 2014; *Shean et al.*, 2016] (DTM credit University of Texas in Table 2). Vertical precision of the DTMs is estimated as: maximum resolution/5/tan(convergence angle) [cf. *Kirk et al.*, 2008]. Vertical precision is generally below 0.5 m and therefore much smaller than the typical depth of the alcoves and the errors associated to vertical DTM precision are therefore negligible compared to the measurements we present here.

For craters that were already dated in other studies we used the ages reported from the literature (Table 1) [*Dickson et al.*, 2009; *Schon et al.*, 2009; *Jones et al.*, 2011; *Johnsson et al.*, 2014; *De Haas et al.*, 2015c; *Viola et al.*, 2015]. The other craters were dated based on the size-frequency distribution of impact craters superposed on the ejecta blanket and rim of the craters using images from the Mars Reconnaissance Orbiter Context Camera (CTX). We defined crater ages based on the crater-size-frequency distribution using the chronology model of *Hartmann*

and Neukum [2001] and the production function of *Ivanov* [2001]. Crater counts were performed using Crater Tools 2.1 [*Kneissl et al.*, 2011], crater-size-frequency statistics were analyzed with Crater Stats 2 [*Michael and Neukum*, 2010]. The diameter range used for the age fits was chosen so as to include as many of the relatively large craters as possible, and to include as many diameter bins as possible, so as to optimize the statistics. We acknowledge that dating impact craters is delicate: the areas of their ejecta blankets can be small, so the number of (especially relatively large) superposed impact craters is generally restricted, and also the number of small craters may be underestimated due to erosion. Therefore, we maintain a large uncertainty range on the crater ages and stress that the reported host crater ages should be interpreted as a range rather than an absolute value (Table 1, Fig. A.1). Most importantly, we explicitly incorporate the age uncertainty range in all analyses, highlighting that the results presented here are insensitive to the age uncertainties.

We use alcove-size as a measure of gully maturity, and compare the size of the gully-alcoves in the study craters using their volume and mean depth (alcove volume divided by alcove area). Gully-alcoves do not exclusively form by the dominant gully-forming mechanism, but are expected to grow in size over time, given persistent gully-forming processes, so that alcove-size provides a proxy for gully maturity. The growth rate of gully-alcoves probably decreases exponentially over time [*De Haas et al.*, 2015c]. Following crater formation, initial alcoves may form by landsliding such that initial rates of alcove weathering, erosion and enlargement are probably large due to the initially highly fractured, oversteepened, and unstable crater wall [e.g,. *Kumar et al.*, 2010; *De Haas et al.*, 2015c]. Over time, the crater wall stabilizes and alcove growth rates will decrease towards more stable and lower background rates. Landsliding and dry rockfalls are expected to contribute to initial gully-growth, but as gullies mature and their alcove gradients decrease, rockfalls will accumulate within alcoves; the gully-forming mechanism is needed to evacuate this debris from the alcoves and to enable further gully growth. *De Haas et al.* [2015c] show that gully-alcoves are substantially larger than non-gullied alcoves (gully-alcoves are larger by a factor 2-60 in Galap, Istok and Gasa craters), implying that a large part of alcove enlargement can be attributed to gully-forming processes, and that gully-alcove size can be used as a proxy for gully maturity. Furthermore, apart from size differences, alcove slopes and drainage patterns also differ substantially between gullied and non-gullied alcoves [e.g., *Conway*, 2010; *Conway et al.*, 2011, 2015].

The volume of material eroded from the alcoves was determined from the elevation models assuming that the ridges surrounding the alcoves (i.e., the alcove watershed) represent the

initial pre-gully surface [cf. *Conway and Balme*, 2014; *De Haas et al.*, 2015a,c]. Alcove volume was then derived by subtracting the original from the pre-gully surface. Such volume estimates are probably conservative, as the volumes are likely to be underestimated as most of the ridges that define the alcove have probably also experienced erosion. In addition, small geometrical errors may arise from digitizing alcove-ridges: error propagation calculations by *Conway and Balme* [2014] suggest that such alcove volume estimates are accurate within 15%. The errors associated with estimating alcove volumes are, however, much smaller than the intra- and inter-crater alcove size variability and therefore do not influence our results.

We categorized craters according to the presence or absence of morphological evidence for (1) present or past glaciation [e.g., *Arfstrom and Hartmann*, 2005; *Head et al.*, 2008; *Levy et al.*, 2009; *Head et al.*, 2010; *Hubbard et al.*, 2011] and (2) mantling by the LDM [e.g., *Mustard et al.*, 2001] (Fig. 2). We identified evidence of past or present glaciation on the walls and floors of craters according to the criteria described by *Head et al.* [2010] and *Levy et al.* [2010b] for lobate debris aprons and concentric crater fill (CCF) (Fig. 2a-b). These criteria include: longitudinal and transverse ridges, troughs and fractures arising from flow deformation and failure of debris-covered ice [*Berman et al.*, 2005, 2009; *Levy et al.*, 2010b]; spatulate depressions at the margins of crater floor-filling materials [*Head et al.*, 2008]; downslope-oriented horseshoe-shaped lobes arising from flow around isolated topographic obstacles; and circular to elongate pits indicative of sublimation of debris-covered ice [*Head et al.*, 2010]. We also classified craters as glaciated if arcuate ridges with similar geometries to those interpreted by *Arfstrom and Hartmann* [2005] and *Hubbard et al.* [2011] as terminal moraines, were present.

We classified craters as containing LDM deposits if meter-to-kilometer-scale topography appeared to be softened by a thin ($\sim$1-10m) drape of smooth or polygonized material [e.g., *Mustard et al.*, 2001; *Kreslavsky and Head*, 2002; *Levy et al.*, 2009] that obscured the underlying fractured bedrock (Fig. 2c-f). We categorized craters as such regardless of the stratigraphic relationship between LDM deposits and the gullies. In some cases, LDM materials partially or completely infilled gully alcoves and other topographic depressions (e.g. small impact craters within the host crater) [e.g., *Christensen*, 2003]. In other cases, gullies incised into LDM deposits [e.g., *Milliken et al.*, 2003; *Conway and Balme*, 2014]. We classified craters as devoid of LDM if pristine gully alcoves were clearly incised into exposed fractured bedrock with no evidence of incision into, or infilling by, a mantling layer. Such alcoves may have been formerly covered by LDM deposits that have subsequently been removed, but have clearly cut substantially into bedrock material and all remnants of LDM are currently gone.

3 Results

3.1 Morphology

In this section the morphology of gullies within the studied craters is divided into three categories, based on their association with LDM and glacial deposits. We describe the morphology of the landforms in the study craters per category. The three morphological categories of landform assemblages we distinguish are: (1) gullies free of LDM and glacial deposits, (2) gullies notably influenced by LDM in the absence of glacial deposits and (3) gullies in association with LDM and glacial deposits. Below we describe the morphology of these types of gully systems in more detail, and divide the studied craters into one of the three categories.

Istok, Gasa and Galap crater contain gullies that are free of LDM and glacial deposits, and which cut directly into the original crater-wall material (Fig. 3) [*Schon et al.*, 2012; *Johnsson et al.*, 2014; *De Haas et al.*, 2015a,b]. These craters host large gully systems on their pole-facing, northern, walls. The largest alcoves are located in the middle of the pole-facing slope and alcoves become progressively smaller in clockwise and counter-clockwise directions. The alcoves have a crenulated shape, indicating headward erosion into the crater rim, and are generally complex, consisting of multiple sub-alcoves. The sharp divides between the alcoves and the upper rims often expose fractured bedrock material, which appears to be highly brecciated and contains many boulders. The alcoves have a very pristine appearance, suggesting that all alcoves have been active recently and there has been little or no infill by secondary processes. The absence of LDM deposits in the gullies is demonstrated by the presence of highly brecciated alcoves hosting many boulders, solely exposing bedrock, the abundance of meter-sized boulders on the depositional fans and the lack of landforms associated with the LDM such as polygonally patterned ground. This does not completely rule out the possibility that these alcoves were formerly covered by LDM deposits that have now been removed, but we would expect in that case remnants of LDM to be recognizable in places. As such, we favor a formation mechanism unrelated to LDM deposits for these gully-systems.

Roseau, Domoni, Tivat and Raga crater encompass gullies that have interacted with and have been influenced by LDM deposits (Fig. 4). Tivat and Raga are small craters (Table 1) and have poorly developed gullies. Tivat contains a single and Raga a few, small-sized, gully systems with elongated alcoves that are sometimes v-shaped in cross-section (Fig. 4). The craters seem covered by a smooth drape of LDM, as shown by the softened appearance of multiple small craters and the presence of patterned ground covering parts of the crater including al-

cove walls. The v-shaped cross-section of many of the gully-alcoves suggests that these alcoves have formed into older mantling material [cf. *Aston et al.*, 2011]. Roseau crater contains well-developed gullies on its pole-facing walls. The gully-alcoves as well as the gully-fan deposits are covered by a smooth drape of LDM material, as implied by the softened appearance of these deposits. All gullies in Roseau crater seem to be covered by LDM material to a similar degree. Domoni crater contains gullies on all crater slopes so there is no preferential gully orientation in this crater. Some gullies in this crater have a fresh appearance, with brecciated alcoves hosting many boulders cutting directly into the original crater-rim material, whereas other neighboring gullies are covered by mantling material (Fig. 4b). This suggests that the gullies in Domoni crater have at least experienced one episode of gully formation (initially unrelated to the LDM), followed by LDM covering and subsequently reactivation of some of the gullies, thereby eroding and removing the LDM from the catchments. This is further supported by the presence of gully-fan lobe surfaces that show different degrees of modification, where the superposed lobes are always the most pristine. The present-day alcoves in Roseau crater and Domoni crater, both those with and without LDM cover, cut directly into the crater rim. Despite the abundance of LDM deposits in Roseau, Domoni, Tivat and Raga crater there is no morphological evidence for the presence of glacial landforms.

The other studied craters show evidence for one or multiple episodes of glaciation (Talu, Flateyri, Taltal, Moni, Artik, Hale, Corozal, Palikir, Nqulu, Langtang, Lyot and Bunnik crater) followed by gully formation (Figs 5, 6). The gullies in these craters are often, at least partly, covered by LDM deposits. There is evidence of substantial ice accumulation having occurred in the past on the crater walls that now host the gullies. This evidence comes in the form of arcuate ridges interpreted as moraine deposits, hummocky deposits from sublimation till remaining from the sublimation and downwasting of glacial ice containing debris, and ridges following the viscous flow patterns of debris-covered glaciers on Mars [cf. *Head et al.*, 2008, 2010]. Although these landforms are located on the lower and shallower slopes of the crater they cannot have formed via glacial processes without the presence of large bodies of ice on the steeper, higher, slopes above. The distribution of the gullies within the craters coincides with the inferred glacial extent. Additionally, the gullies that form in the hollows of formerly glaciated crater walls do not extend up to the crater rim and are often elongated to v-shaped, suggesting incision into ice-rich, unlithified, sediments [*Aston et al.*, 2011]. The gullies superpose and postdate the glacial deposits, and thus formed following recession of the glaciers. In some craters the tops of former alcoves are still visible on the crater wall.

A typical example of this can be found in Langtang crater (Fig. 5). These alcoves are likely the remnants of former gully alcoves, which may have been excavated and enlarged by glacial activity [cf. *Arfstrom and Hartmann*, 2005]. Glacier(s) may have formed within the old gully alcoves, thereby creating a broader glacial alcove and enlarging the former gully alcove, potentially explaining the relatively broad and smooth appearance of the alcoves. The extent of sublimation-till deposits provides evidence for a major episode of glaciation in Langtang crater, whereas moraine deposits define the extent of a younger, smaller, glacial episode (Fig. 5). The pitted lobate sublimation till deposit which extends $\sim$1.5 km across the northern portion of the floor of Langtang crater may be the remnant of an LDA which formed during a major episode of glaciation. Spatulate depressions with raised rims within this deposit at the base of the crater wall are similar to those interpreted by *Head et al.* [2008] as troughs carved by the more recent invasion of pre-existing deposits on the crater floor by smaller glacial lobes, which advanced down the crater wall and were subsequently removed by sublimation. Along the crater rim the crowns of alcoves that cannot be directly related to gully-fans are visible. Below these alcoves, younger alcoves have cut into the crater wall. These younger alcoves are connected to gully-fans, whereas the fan deposits associated to the older generation of alcoves are not visible anymore. These deposits may have been overridden by younger glaciers that have been present within the crater, although this remains speculative as there is no evidence of glacial deposits superposing older gully deposits apart from the possible remnants of older alcoves.

In Bunnik crater there is evidence for at least two different generations of alcoves (stage 1 and 2), and potentially for four generations of alcoves (stage 3 and 4) (Fig. 6). These generations can be distinguished based on cross-cutting relationships and degree of degradation. The youngest (stage 1) alcoves have cut up to 25 m deep into a thick layer of LDM deposits that occupy the hollows of older, stage 2, alcoves, demonstrated by their elongated shape and abundance of polygonal patterned ground [*Conway and Balme*, 2014]. In front of the gully-fans, just below the youngest alcoves, a complex of ridges is present, which may mark the extent of former ice accumulation. Below these systems there is a relatively gently sloping apron (5-10°) composed of juxtaposed degraded cone-shaped deposits. These deposits are much younger than the crater floor given the marked difference in abundance of superposed craters. We interpret these deposits to be the remnants of large inactive fans given their slope and cone shape. This interpretation is supported by the absence of morphologies indicative of flow deformation or volatile loss [e.g., *Head et al.*, 2010], which leads us to exclude a glacial origin for these

deposits. These fan deposits might have originated from the large abandoned alcoves of stage 3 and 4.

3.2 Crater age versus and gully size and landform assemblage

The craters studied here range in age from <1 Ma up to multiple billion years (Table 1, Fig.A.1). Figure 7 shows the relation between host crater age and alcove volume and mean alcove depth for the active alcoves of the gullies in the craters studied here. The size of the alcoves has a similar range in all craters regardless of crater age, implying that there is a mechanism that limits gully size over time. Notably, gullies in even the youngest craters are similar in size to those present in craters of billions of years old. To explain this, we subdivide the gullies into the three morphological categories described in the previous section. From this analysis it becomes clear that the youngest craters host gullies that are unaffected by LDM or glacial episodes, whereas the LDM and glacial influence increases with crater age. The oldest crater unaffected by LDM and glacial deposits is Galap crater (best-fit age 6.5 Ma; 5-9 Ma uncertainty range). Roseau crater (best-fit age 2.8 Ma; 2-4 Ma uncertainty range) is the youngest crater affected by LDM deposits, whereas Talu crater (best-fit age 14 Ma; 10-22 Ma uncertainty range) is the youngest crater in our dataset to have been affected by glaciation. In contrast, the other three craters within the same age range (∼10-50 Ma: Domonik, Tivat and Raga) are affected by LDM deposits, but not by glaciers. The older craters in our dataset (>50 Ma) have all been affected by the LDM and glaciation. Moreover, potential evidence for multiple episodes of activity, by the presence of multiple generations of alcoves is mainly found in the oldest craters (see for example Figs 5 and 6).

Artik crater provides quantitative evidence for very recent gully deposits in a much older host crater. Artik crater is covered with secondaries from the Gasa crater impact, which provide a chronological marker event inside Artik crater at ∼1.25 Ma (Fig. 8) [*Schon et al.*, 2009; *Schon and Head*, 2011]. Gasa crater is located ∼100 km to the southwest of Artik crater. The alcoves of the gullies in Artik crater cut in LDM material as indicated by their elongated shape [*Schon and Head*, 2011]. The presence of an arcuate ridge in front of the gully-fan suggests former ice accumulation and potentially glacial activity. The oldest gully-fan lobe of the major gully complex is superposed by Gasa secondaries, implying that its formation predates Gasa impact, whereas the younger gully-fan lobes are free of secondaries and therefore postdate the formation of Gasa crater [*Schon et al.*, 2009; *De Haas et al.*, 2013]. This shows that the gul-

lies in Artik crater are less than a few million years old. Artik crater itself formed ∼590 Ma (uncertainty range 300 Ma - 1 Ga) and is therefore much older than the gullies.

4 Discussion

4.1 Model of the temporal evolution of gullies

The close association between the distribution of gullies and the extent of former glaciers, the evidence for glacial emplacement and multiple generations of alcoves in some locations, and the crosscutting relations between glacial landforms and gullies suggest an intimate link between glaciation and gully formation in the studied craters, with glaciers potentially removing or burying gully deposits but potentially also providing volatiles for new gully formation after deglaciation. By combining crater age with these observations of gully morphology and associated landform assemblages as discussed here and in literature, we provide the following conceptual model for the temporal evolution of gullies on Mars (Fig. 9):

(1) Following crater formation gullies may develop in midlatitude to polar craters. The mechanism by which these gullies form depends on the climatic conditions during crater formation. If obliquity allows snow/ice accumulation in alcoves the gullies may predominantly form by aqueous processes, whereas alternatively they may perhaps predominantly form by dry processes, likely involving CO_2, during periods where snow/ice does not accumulate or melt. Following crater formation initial rates of geomorphic activity are typically high, because the interior parts of crater rims are generally oversteepened shortly after their formation and consist of highly faulted, fractured and fragmented materials [e.g., *Kumar et al.*, 2010]. As a result they are particularly prone to weathering, enabling rapid growth of alcoves and providing ample sediment to be transported to gully-aprons ['paracratering' effect; see *De Haas et al.*, 2015c, for a more extensive description of this effect]. Gullies may therefore rapidly form in fresh craters, which may explain the vast gully systems that have formed in Istok and Gasa crater within ∼1 Myr (Fig. 3).

(2) Over time the crater wall stabilizes and as a result geomorphic activity, and thus gully growth, decreases [cf. *De Haas et al.*, 2015c]. If obliquity is high enough for LDM deposition to occur, LDM deposits may accumulate in gully alcoves. When LDM covers gullies, bedrock alcoves are protected from weathering and geomorphic flows will largely result in mobilization and transport of the clastic material present in the LDM [*De Haas et al.*, 2015b]. Geomorphic flows will therefore hardly erode the original crater-wall surface or talus slope. As

a result, there will be little or no net gully-alcove growth. Evidence for cyclical LDM accumulation-degradation and interactions thereof with gullies have also been observed and described in detail by *Dickson et al.* [2015].

(3) When mean obliquity is high and local conditions allow sufficient accumulation of snow/ice on the interior wall of an impact crater and in gully-alcoves, glaciers may develop. As glaciers grow and flow down the crater wall, they may override and obscure or remove older deposits on the crater wall and within the crater. Only the upper parts of alcoves (crowns) may generally be preserved on the crater wall (Figs 5, 6), although distal fan deposits may be preserved when glaciers do not reach far enough downslope (Fig. 6). For the rest, the removal or burial of former gully deposits by glacial activity can only be hypothesized, given the lack of preserved old gully deposits below glacial features.

(4) When mean obliquity decreases and the glaciers sublimate and potentially melt, a smoothed crater wall becomes exposed whereon former gully deposits have been largely removed or obscured. Deglaciation exposes an oversteepened crater wall, which is likely highly fractured due to enhanced stress relaxation caused by debuttressing (removal of the support of adjacent glacier ice) [e.g., *Ballantyne*, 2002]. Moreover, sublimation or melting of a glacier will leave abundant loose sediment behind, which was formerly within or on top op the glacier ice. This will lead to enhanced geomorphic activity on a crater wall following deglaciation, decreasing to a background rate over time [‘paraglacial’ effect; *Church and Ryder*, 1972]. Gullies may thus rapidly form and develop following deglaciation (similar to the enhanced gully growth after crater formation), especially as melt of former glacial ice may cause debris flows and fluvial flows [*Head et al.*, 2008].

(5) The gully formation/degradation cycles may repeat themselves (between the above described phases 2 and 4) if time and environmental conditions allow.

In short, gullies develop rapidly following crater formation or deglaciation. If time and local conditions permit, they may subsequently go through formation/degradation cycles driven by (1) LDM emplacement and degradation and by (2) glacial emplacement and removal. The former cycles are probably more common, whereas the latter cycles have a stronger effect on the gullies as they may completely remove or bury gully deposits. These cycles limit gully-size and -age, explaining their pristine appearance.

4.2 Timing and link to obliquity cycles

The current obliquity of Mars is ∼25° but obliquity has been greater in the past. During the last 250 Ma obliquity values likely ranged from 0° to 65° [*Laskar et al.*, 2004]. From 21 to 5 Ma obliquity ranged between 25° and 45° around an average obliquity of 35° (Fig. 10), while from 5 Ma to present-day obliquity dropped to a mean of 25°, varying between 15° and 35°. These obliquity variations have inevitably had large effects on the Martian climate and water cycle, and have likely caused alternating glacial and interglacial periods in the past [e.g., *Head et al.*, 2003; *Forget et al.*, 2006].

The obliquity threshold for snow and ice transfer to the midlatitudes has been estimated to be 30° [e.g., *Head et al.*, 2003]. The threshold for melting and associated morphological activity is probably higher but unknown [*Williams et al.*, 2009], likely in the 30-35° obliquity range [*De Haas et al.*, 2015a]. However, *Kreslavsky et al.* [2008] suggest that an active permafrost layer has not been present on Mars in the last ∼5 Ma when mean obliquity was relatively low, because insufficient ground ice was able to melt. Using a global circulation model *Madeleine et al.* [2014] predict annual snow/ice accumulations of ∼10 cm in the midlatitudes at 35° obliquity. Melting of such quantities of snow would probably be sufficient to cause substantial flows in gullies, especially as snow is being trapped and collected in alcoves [*Christiansen*, 1998]. It would, however, probably be insufficient for the formation of glaciers, especially as most snow is predicted to sublimate at 35° obliquity [*Williams et al.*, 2009]. Global circulation models show that sufficient amounts of ice may be moved towards the midlatitudes to cause midlatitude glaciation, during transitions from high ∼40-45° to moderate obliquity of 25-35° [e.g., *Levrard et al.*, 2007; *Madeleine et al.*, 2009]. High mean obliquity (∼45°) results in accumulation of tropical mountain glaciers at the expense of polar reservoirs. A subsequent transition to moderate (∼35°) obliquity would increase equatorial insolation, mobilize equatorial ice and drive deposition of large volumes of ice in the midlatitudes. In the midlatitude regions, this ice is likely to accumulate on plateaus and in alcoves and flow down-slope to form glacial systems [e.g., *Baker et al.*, 2010]. Accordingly, *Head et al.* [2008] suggest that higher obliquities led to more water in the atmosphere in the midlatitudes and deposition of snow and ice, particularly in favored and shielded microenvironments such as pole-facing crater interiors at these latitudes.

These hypothesized thresholds and models for snow and ice transfer to the midlatitudes, melting and glaciation correspond well with our observations on combined crater age and mor-

phology (Fig. 10). The three craters without any evidence for LDM or glaciation formed within the last 5 Ma, and thus fall within the period of relatively low mean obliquity (Istok and Gasa) or at the end of the last high mean obliquity period (Galap). The estimated age of Istok crater is younger than the termination of the most recent mantling episode ∼0.4 Myr age [*Head et al.*, 2003; *Smith et al.*, 2016], explaining the lack of LDM deposits. The timing of the termination of the most recent mantling episode may vary with latitude, however, and may have finished earlier at lower latitudes. Gasa and Galap crater have likely experienced multiple >30° obliquity periods, suggesting that LDM deposition may have occurred in these craters given their location within the southern midlatitude band. The apparent absence of LDM deposits in these craters may be because LDM was never deposited in Gasa and Galap craters, which might be possible given their relatively low latitudes of 35.7° S and 37.7° S, respectively. Alternatively, the LDM deposits emplaced in these craters were too thin to be preserved and too thin to significantly affect gully formation. The age of ∼2.8 Ma of the youngest crater covered by LDM deposits, Roseau crater (latitude 41.7° S), is consistent with temporal constraints on the latest episode of LDM deposition by *Schon et al.* [2012]. The older craters that have all been exposed to high mean obliquity for a substantial time period show evidence of LDM accumulation and glacial activity. Talu crater is the youngest crater that hosts viscous flow features. Its age of 10-22 Ma suggests that glacial landforms can develop on relatively recent timescales, at least locally, as the other three craters with the same age show evidence for LDM deposition but not for glaciation. The older craters, all 300 Ma or older, show evidence for LDM and glaciation as would be expected because these craters have experienced multiple and long episodes of high obliquity [*Laskar et al.*, 2004].

This temporal trend is in good agreement with the inferred timing of glacial activity in the Martian midlatitudes. Dating of glacial landforms, such as lobate debris aprons and lineated valley fill, provide evidence for large-scale glacial episodes in the northern and southern midlatitudes within the last ∼100 million to billion years on Mars [e.g., *Dickson et al.*, 2008; *Baker et al.*, 2010; *Hartmann et al.*, 2014; *Fassett et al.*, 2014; *Baker and Head*, 2015; *Berman et al.*, 2015]. Smaller-scale glacier-like forms have probably been active more recently, for example small-scale lobate glaciers in Greg crater (38.5° S, 113° E) have been dated to have been active 10-40 My ago [*Hartmann et al.*, 2014]. Such relatively small lobate debris-covered glaciers are of a similar scale as the systems that formed the possible moraine deposits that are present below gullies in some of the craters studied here, and their timing corresponds well with the timing of the most recent glacial episode that we found in Talu crater. The end of this latest

glacial episode marks the start of the gully formation on crater walls formerly occupied by viscous-flow features and glacial deposits, and is distinct from the much larger glacial events of >100 Ma. The presence of multiple glacial episodes on Mars, and their interaction with gullies, raises the question how many glacial/post-glacial cycles have modified Amazonian landscapes on Mars.

4.3 Paleoclimatic implications

The morphological evidence for one or more cycles of gully activity and the good correlation between the number and extent of these cycles and host crater age is in agreement with previous findings that Mars has undergone numerous climatic changes, likely forced by orbital variations [e.g., *Head et al.*, 2003; *Smith et al.*, 2016].

The association between LDM, glacial activity and gully-activity in many Martian craters suggests that the abundance of water-ice has influenced the evolution of gullies in glaciated landscapes on Mars. Water ice is the main component of the LDM and glacial deposits, and the extent of former glaciers is generally strongly correlated with the distribution of gullies. This suggests that gully formation may be linked to glacial activity, further suggesting that some gullies may have formed by melting of ice within the LDM or glacial deposits. On the other hand, the large gully-systems in the very young Istok, Gasa and Galap craters, which are free of LDM and glacial deposits, show that extensive gully activity may also occur in the absence of LDM and glacial deposits. These gullies may have formed by aqueous flows, dry CO_2-triggered flows, or a combination as follows. Obliquity has hardly exceeded 35° since the formation of Istok, Gasa and Galap craters, which may explain the absence of LDM and glacial features in these craters. Nevertheless, obliquity may have been sufficiently high for snow accumulation and melting in alcoves [e.g., *Head et al.*, 2008; *Williams et al.*, 2009], resulting in aqueous gully-activity [*De Haas et al.*, 2015a]. Such a mechanism is supported by the morphology of the gully-fan deposits in Istok crater which closely resemble aqueous debris flows on Earth [*Johnsson et al.*, 2014; *De Haas et al.*, 2015a]. Additionally, the sedimentology in vertical walls along incised gully-channels and gully morphometry in Galap crater are consistent with predominant formation by debris flows [*De Haas et al.*, 2015b]. Gasa crater formed inside a larger host crater, impacting into the remnants of debris-covered glaciers formed earlier in the Amazonian. *Schon and Head* [2012] suggest that the Gasa impact penetrated into the southern portion of this glacier, and that this ice provided a source of meltwater that formed the gullies in Gasa crater. Slope stability analyses on the gully-alcoves in Gasa crater indeed suggest that liquid H_2O was present in the formation of the gully-alcoves [*Okubo et al.*, 2011].

Moreover, morphometric analyses performed by *Conway and Balme* [2016] imply that the gullies in these craters have been carved by liquid water. On the other hand, the regions where H_2O is expected to accumulate are likely the same regions where CO_2 may be expected to accumulate, and present-day gully activity related to CO_2 frost has been observed to modify gullies in Gasa crater [*Dundas et al.*, 2010]. *Dundas et al.* [2010] observed movement of meter-scale boulders and topographic changes in two separate channels and aprons, showing that sediment transport in the gullies in Gasa crater is ongoing today. Additionally, recent smaller-scale gully activity that may be related to CO_2 frost has amongst others been observed in Palikir crater [*Dundas et al.*, 2012; *Vincendon*, 2015] and Corozal crater [*Dundas et al.*, 2010, 2015; *Vincendon*, 2015]. These are both old craters (Corozal $\sim$500 Ma; Palikir $\sim$2.8 Ga) hosting evidence for former glaciation, which shows that even if the distribution of gullies is strongly correlated to former glacial deposits their formative mechanisms might not be uniquely related to liquid water. However, multiple processes acting simultaneously, sequentially, or cyclically within the same steep catchment or chute on Earth is normal [e.g., *Blair and McPherson*, 2009]. Hence, finding evidence for dry mass wasting within a steep gully chute is far from definitive evidence of gully formation by dry processes only.

In short, these observations cannot determine whether aqueous or CO_2-triggered flows contributed most substantially to gully formation. Yet, the intimate relation between LDM, glacial deposits and gully deposits in older craters suggest the presence of periods wherein liquid water plays an important role in gully formation. The observed relation between gullies and LDM and glacial deposits shows that ice is abundant on many Martian midlatitude and polar crater walls during glacial episodes, and that melting of this reservoir is consistent with the observed stratigraphy. Further research would be needed to evaluate the potential of CO_2 to (partly) explain these stratigraphic relationships. The Martian climate has varied substantially over time, and it is likely that the processes of gully formation and modification may have varied accordingly.

4.4 Potential spatial variations

The present study is a first attempt to quantitatively study the temporal evolution of Martian gullies. Although we have used all publicly available HiRISE DTMs that host gullies and for which host crater dating was possible, and even extended these with 8 of our own DTMs this study is based on gullies in 19 craters only. Therefore, we can hardly take into account any local and/or spatial effects on the temporal evolution of gullies. These are, however, prob-

ably important as there is a strong latitudinal control on the distribution and orientation of Martian gullies [e.g., *Balme et al.*, 2006; *Dickson et al.*, 2007; *Kneissl et al.*, 2010; *Harrison et al.*, 2015] and LDM and glacial deposits [e.g., *Squyres*, 1979; *Milliken et al.*, 2003; *Head et al.*, 2003; *Souness et al.*, 2012; *Brough et al.*, 2016]. Moreover, *Dickson et al.* [2015] show that there is a latitudinal control on the interaction between LDM deposition, removal and gully activity. They suggest that in the lower midlatitudes (30-40°) gullies go through cyclical degradation and removal, whereas gullies go through cycles of burial and exhumation of inverted gully channels in the transitional latitude band between dissected and preserved LDM (40-50°). The study by *Dickson et al.* [2015] focuses on LDM-hosted gullies, however, and does not consider gullies with alcoves that incise into bedrock, in contrast to this study.

To further explore the spatial imprint on the temporal evolution of Martian gullies, the quantitative temporal dataset presented here needs to be extended. A larger quantitative temporal dataset may ultimately enable separating spatial and temporal trends, which will further enhance our understanding of the spatio-temporal evolution of Martian gullies and may ultimately advance our understanding of their formation processes and the role of volatiles therein. Moreover, with a larger sample size, latitudinal variations in the present-day state of glaciation on Mars and their relation with gullies may potentially serve as analogues for temporal variations [i.e., the concept of space-for-time substitution; *Pickett*, 1989].

5 Conclusions

This paper quantitatively constrains and explains the temporal evolution of Martian gullies. To this end, the size of gullies, determined from HiRISE elevation models, and the relation between gullies, LDM deposits and glacial deposits are compared with host crater age in 19 craters on Mars.

Our results indicate that the size of gullies is unrelated to host crater age. Gully-size in very young host craters of a few million years old is similar to gully size in old host craters over a billion years old. Gullies on the walls of very young impact craters are free of LDM deposits ($<$ a few Myr old), whereas they become increasingly influenced by LDM and glacial activity with increasing crater age. Gullies in craters of a few million to few tens of millions years old are typically affected by the LDM but not by glacial activity, while gullies in host craters of a few tens of millions years old or older are generally affected by both the LDM and glacial deposits.

These observations suggest that, after their formation in fresh craters, gullies may go through repeated sequences of (1) LDM deposition and reactivation and (2) glacier formation and removal, and the formation of new gully systems. Both sequences are likely governed by obliquity-driven climate changes and may limit gully growth and remove or bury entire gully-fan deposits, thereby explaining the similar size of gullies in young and old host craters.

The temporal evolution of gullies can be summarized as follows. Following crater formation gullies may rapidly form on the highly-fractured and oversteepened walls of the fresh impact crater. Over time, the crater wall stabilizes and rates of geomorphic activity and gully growth decrease. When obliquity is favorable, there is LDM deposition on top of the gullies, which largely hampers further gully-alcove growth into bedrock mainly because geomorphic flows now originate from the LDM deposits rather than the original crater-wall material. There may be several sequences of LDM removal and deposition, until local conditions allow for sufficient accumulation of snow/ice on the gullied crater-wall for the formation of glaciers. These glaciers probably remove or bury the gully deposits, and leave behind a smoothed, oversteepened, crater wall rich in loose material after their retreat. The crater wall conditions following glacier retreat favor enhanced rates of geomorphic activity and enable rapid growth of new gullies and if time permits the above described sequence of gully evolution may repeat itself.

The association between LDM, glaciers and gullies suggests a strong control of water on the evolution of gullies. Meltwater of LDM and glaciers may have resulted in gully-formation by aqueous flows, especially as the distribution of gullies often closely coincides with the extent of former glaciers. Yet, the role of liquid water remains debatable, as present-day gully activity unrelated to liquid water is observed in some of the gullies formed after retreat of glaciers and in the absence of LDM and glacial deposits in the youngest gullied craters in our dataset. The Martian climate has varied substantially over time, and the dominant gully-forming mechanisms likely varied accordingly.

Acknowledgments

Reviewers will be thanked. TdH is funded by the Netherlands Organization for Scientific Research (NWO) via Rubicon grant 019.153LW.002. SJC and MRB are funded by a Leverhulme Trust grant RPG-397. MRB was supported also by the UK Space Agency (Grant ST/L00643X/1) and the UK Science and Technology Facilities Council (grant ST/L000776/1). FEGB is funded by STFC grant ST/N50421X/1. PMG is funded by the UK Space Agency (grant ST/L000254X/1),

and acknowledges the UK NASA RPIF at University College London for DTM processing facilities.

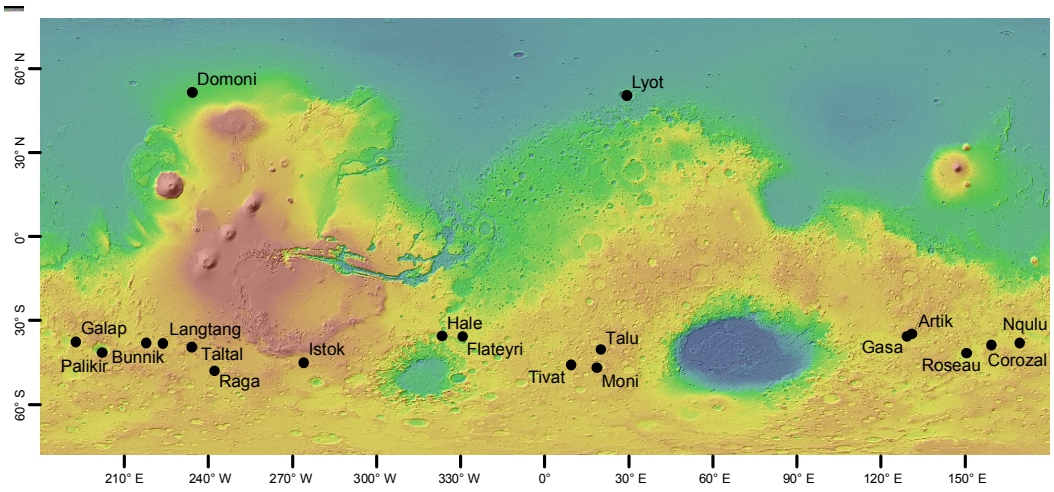

572 **Figure 1.** Study crater locations. Background, color-keyed and relief-shaded, topography is from the Mars
573 Orbiter Laser Altimeter (MOLA, red is high elevation, blue is low elevation).

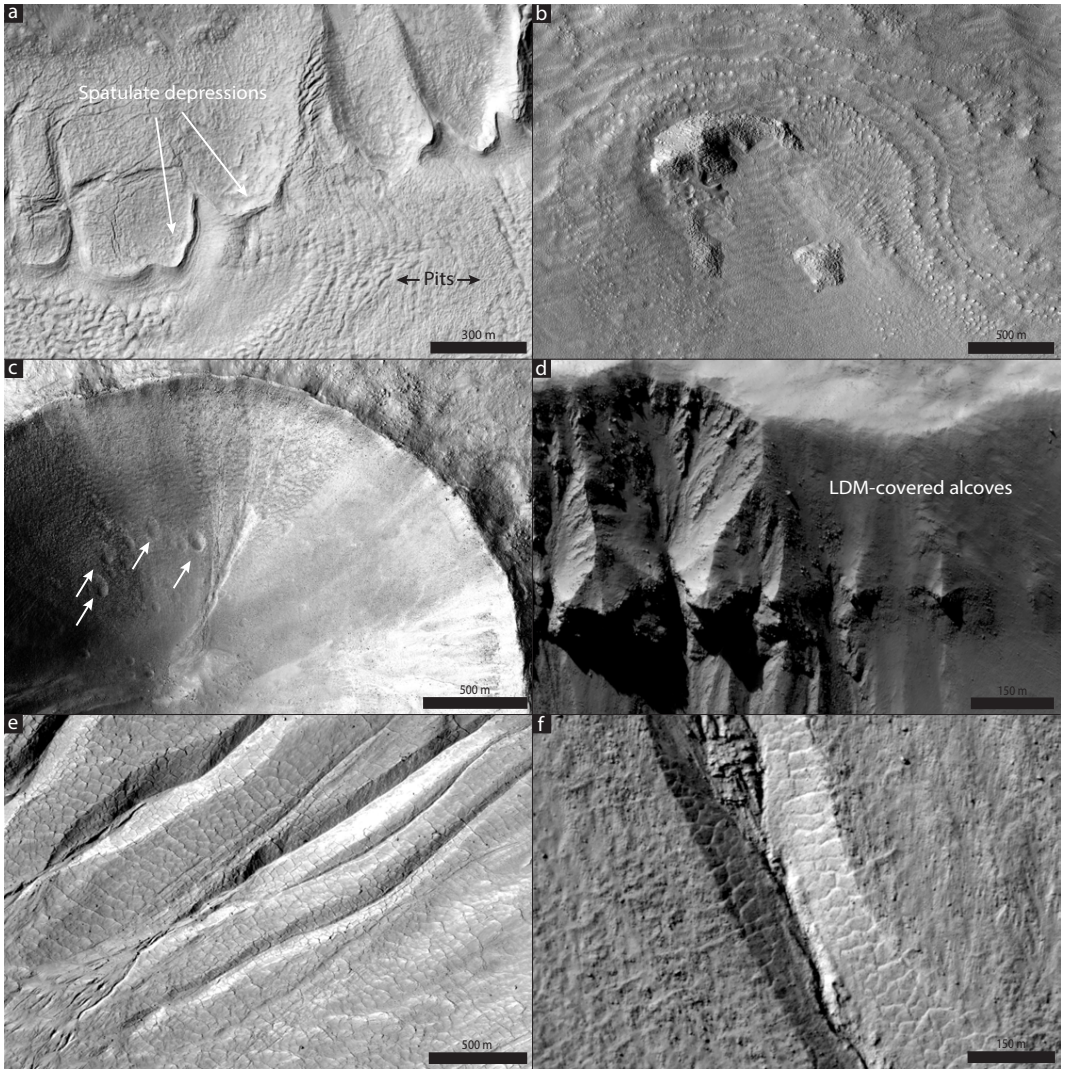

574 **Figure 2.** Examples of morphological evidence used to classify craters as influenced by the latitude-
575 dependent mantle and/or influenced by past or present glaciation: (a) Arcuate spatulate depressions, which we
576 interpret as moraine deposits, at the headward margin of an LDA on the floor of Langtang crater. Circular to
577 elongate pits on the surface of the LDA support an ice-rich composition (HiRISE image ESP_023809_1415).
578 (b) Horseshoe-shaped viscous flow around a topographic obstacle on the floor of Talu crater. Sub-parallel
579 ridges near to the margins of the flow are consistent with a compressional regime within flowing ice
580 (HiRISE image ESP_011672_1395). (c) Softening of topography in the interior of Tivat crater by LDM
581 materials that partially infill small impact craters (white arrows) on the interior crater wall (HiRISE image
582 ESP_012991_1335). *Levy et al.* [2009] suggest that the gullies on this crater wall formed within the LDM
583 deposits. (d) Infilling and softening of gully topography in Domoni crater by accumulations of LDM. The
584 mantle obscures the fractured bedrock into which the unmantled gullies (on the left of the panel) are incised
585 (HiRISE image ESP_016213_2315). (e) Pervasively polygonized LDM materials incised by gullies on the
586 wall of Talu crater (HiRISE image ESP_011672_1395). (f) Polygonized walls of a gully alcove in Langtang
587 crater, providing evidence for gully incision into an ice-rich mantle (HiRISE image ESP_023809_1415).

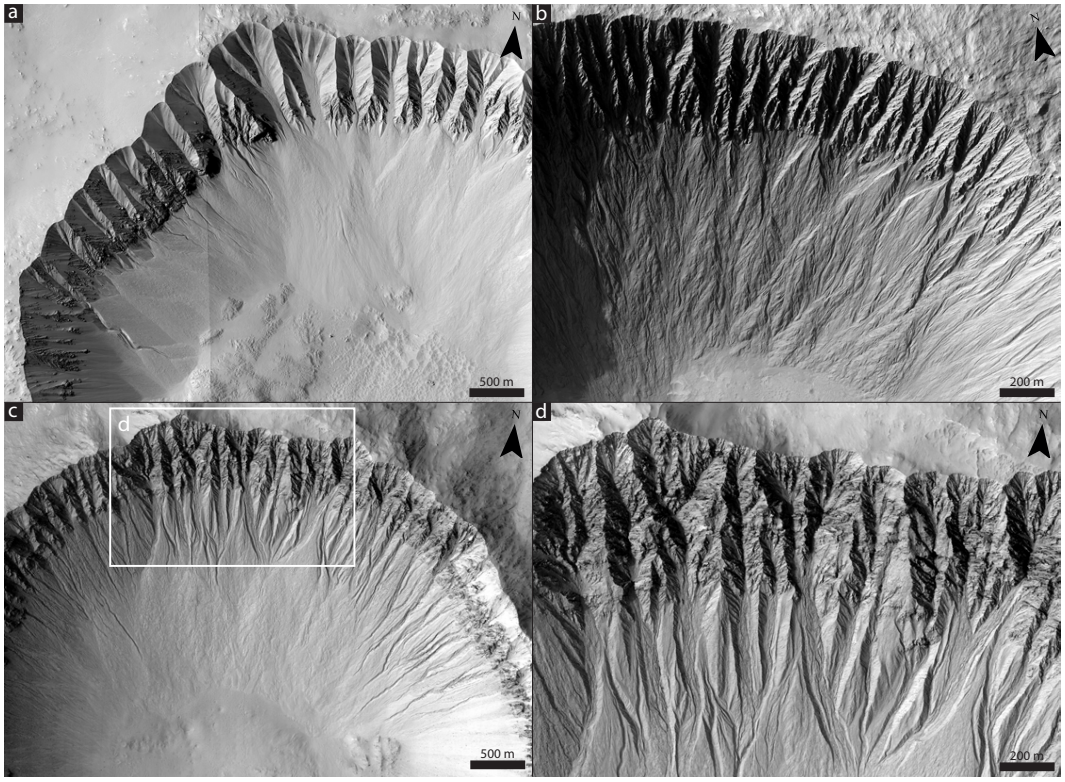

588 **Figure 3.** Morphology of young craters. The gully-alcoves have a crenulated shape and cut into the
589 upper crater rim, exposing fractured and highly brecciated bedrock containing many boulders. (a) Gasa
590 crater (HiRISE images ESP_014081_1440 and ESP_021584_1440). (b) Istok crater (HiRISE image
591 PSP_006837_1345). (c) Galap crater (HiRISE image ESP_012549_1420). (d) Detail of Galap crater alcoves.

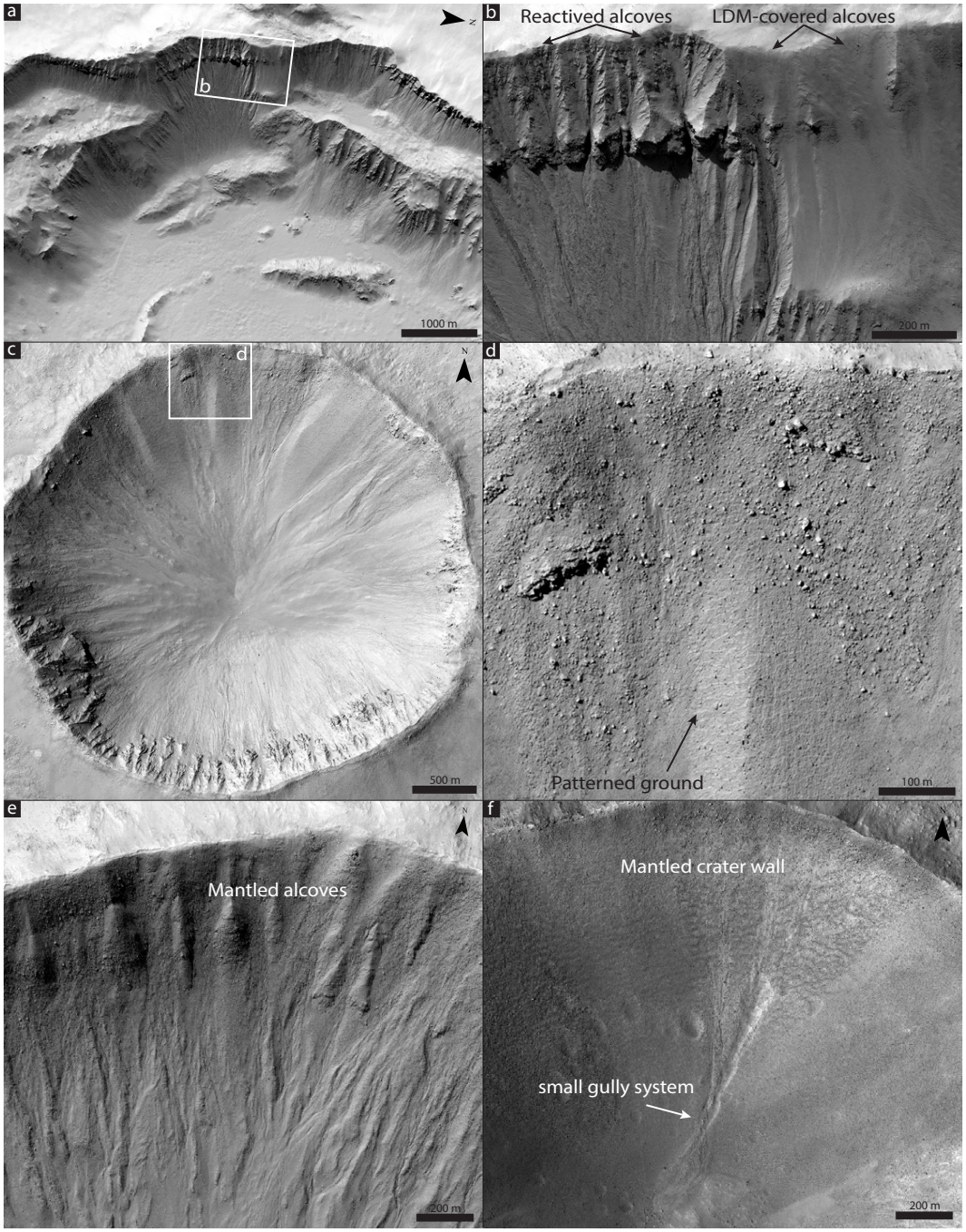

592 **Figure 4.** Interaction between gullies and LDM in Domoni, Raga, Roseau and Tivat craters. (a) West-
593 ern wall of Domoni with abundant gullies. Evidence for former glaciation is absent (HiRISE image:
594 ESP_016714_2315). (b) Detail of gully-alcoves: the gully-alcoves in the right side of the images are cov-
595 ered by LDM deposits, whereas the gully-alcoves on the left side of the image have been reactivated since the
596 last episode of LDM emplaced and therefore these alcoves are largely to completely free of LDM deposits.
597 (c) Raga crater (HiRISE image: ESP_014011_1315). (d) Detail of gully-alcoves in Raga crater with soft-
598 ened topography and patterned ground. (e) Detail of pole-facing gullies covered by LDM deposits in Roseau
599 crater (HiRISE image: ESP_024115_1380). (f) Mantled pole-facing wall of Tivat crater (HiRISE image:
600 ESP_012991_1335).

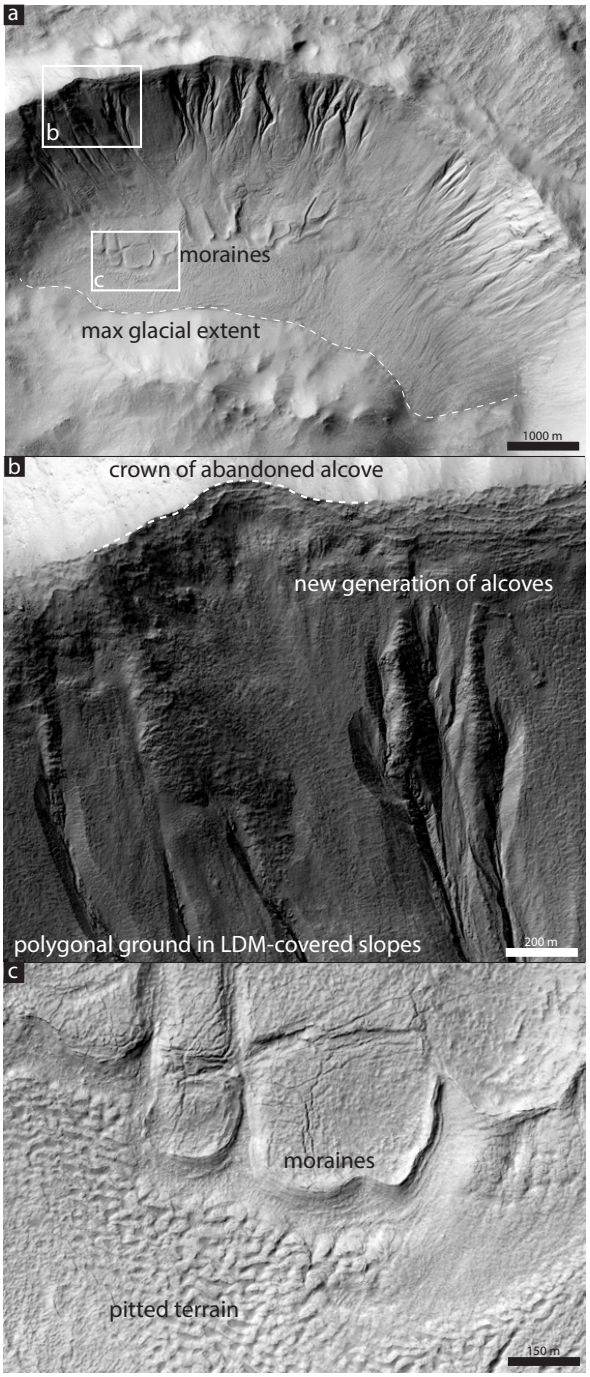

Figure 5. Multiple generations of alcoves and glacial advances in Langtang crater. (a) Glacial extent. CTX image F10_039752_1419_XI_38S142W. (b) Detail of the crater slope, showing the crown of a former, now abandoned, alcove and younger smaller generations of alcoves. The crater slope is covered by a thick layer of ice-rich material, as demonstrated by the shape of the youngest alcove incisions and polygonal patterned ground on top of the crater wall. The new alcove incises by more than 25 m into the crater wall. HiRISE image: ESP_023809_1415. (c) Detail of the moraine deposits and the pitted terrain, which originates from sublimation till. HiRISE image: ESP_023809_1415.

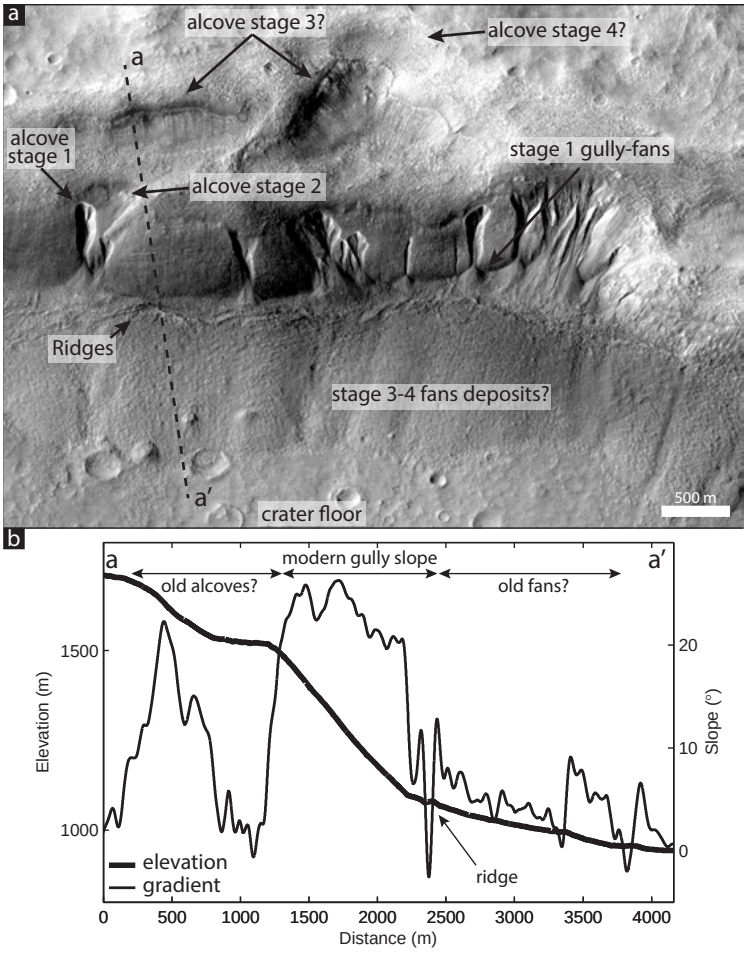

608 **Figure 6.** Multiple alcove and fan generations in Bunnik crater. (a) At least two generations of alcoves
609 (stage 1 and 2), and potentially four generations of alcoves (stage 3 and 4), can be recognized on the crater
610 wall. Below the youngest gullies (stage 1) arcuate ridges can be identified, under which the remnants of the
611 lower parts of extensive fans can be recognized (note the difference in amount of superposed craters on these
612 fan deposits and the crater floor). CTX image F10_039752_1419_XI_38S142W. (b) Elevation and gradient
613 along line a-a'.

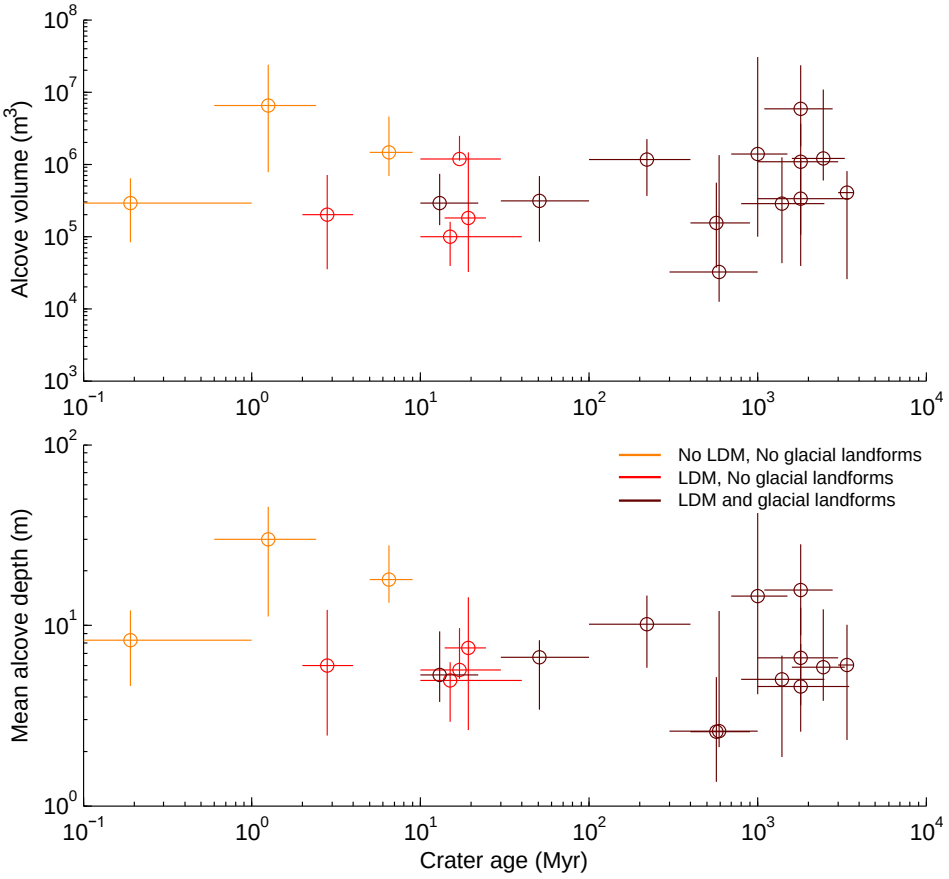

Figure 7. Gully-alcove size as a function of crater age. (a) Crater age versus alcove volume. (b) Crater age versus mean alcove depth. The circles are the best fit crater ages and the median backweathering rates per crater. Bars denote minimum and maximum crater age and the 10th and 90th percentile alcove size of the measured gully-alcoves within each crater.

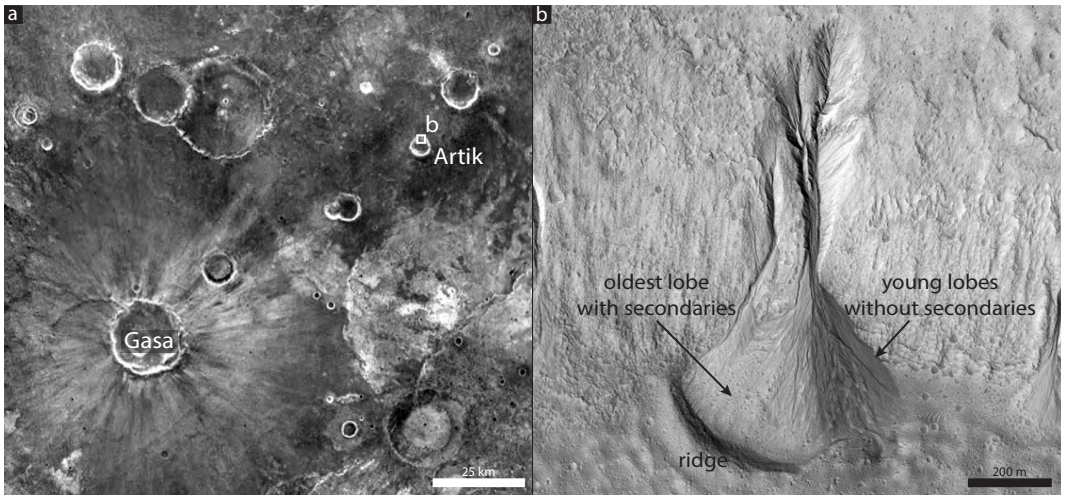

Figure 8. Artik crater (∼590 Ma). (a) Themis nighttime infrared image showing the distribution of the Gasa impact rays from which the large population of secondaries in Artik crater originate. (b) Gully in Artik crater. The oldest lobe of the crater is covered by secondaries and thus older than 1.25 Ma, whereas the superposed gully-fan lobes are free of secondaries and are thus younger than 1.25 Ma [cf. *Schon et al.*, 2009; *De Haas et al.*, 2013] (HiRISE image: ESP_012314_1450).

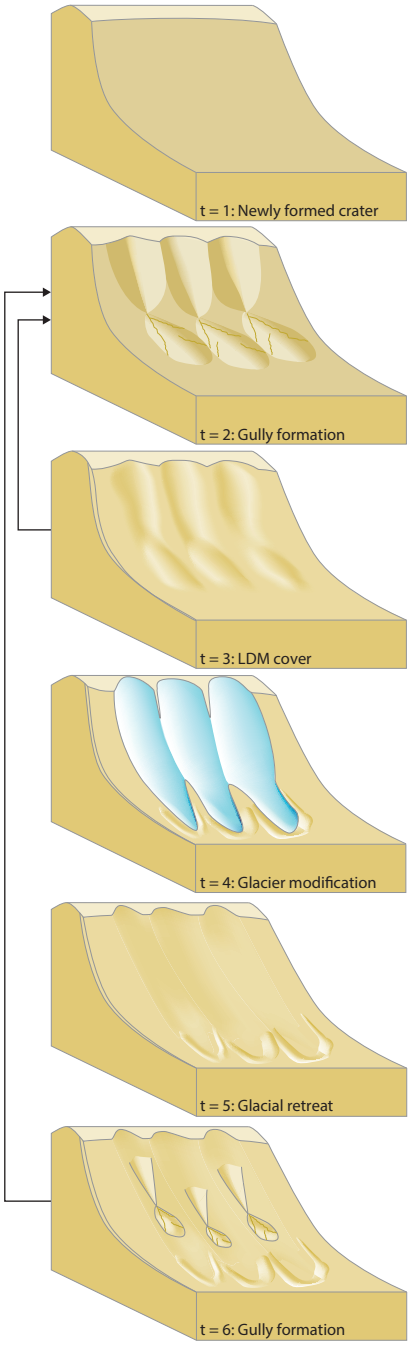

Figure 9. Conceptual model of the temporal evolution of gullies on Mars. (t=1) The highly-fractured and unstable walls of newly formed impact craters are prone to gully formation. (t=2) As a result, large gullies may rapidly form. Such gullies may typically cut into the crater rim. (t=3) During high-obliquity periods the gullies may be covered by LDM deposits, which impedes further gully-alcove growth. Subsequently, gullies may reactive and transport the LDM deposits in the gully alcoves to the gully-fan until a new mantling episode commences. Gullies may experience multiple repeats of these cycles. (t=4) During favorable obliquity periods glaciers may form on the crater wall removing or burying the gully deposits, and forming a moraine deposit at the toe of glacier. (t=5) Following glacial retreat a smoothed crater wall and moraine deposits remain. (t=6) New gullies may now form within the formerly glaciated crater wall. Such gullies typically have v-shaped and elongated alcoves and do not extend to the top of the crater wall. The gullies may enlarge until there is another episode of LDM emplacement or glaciation.

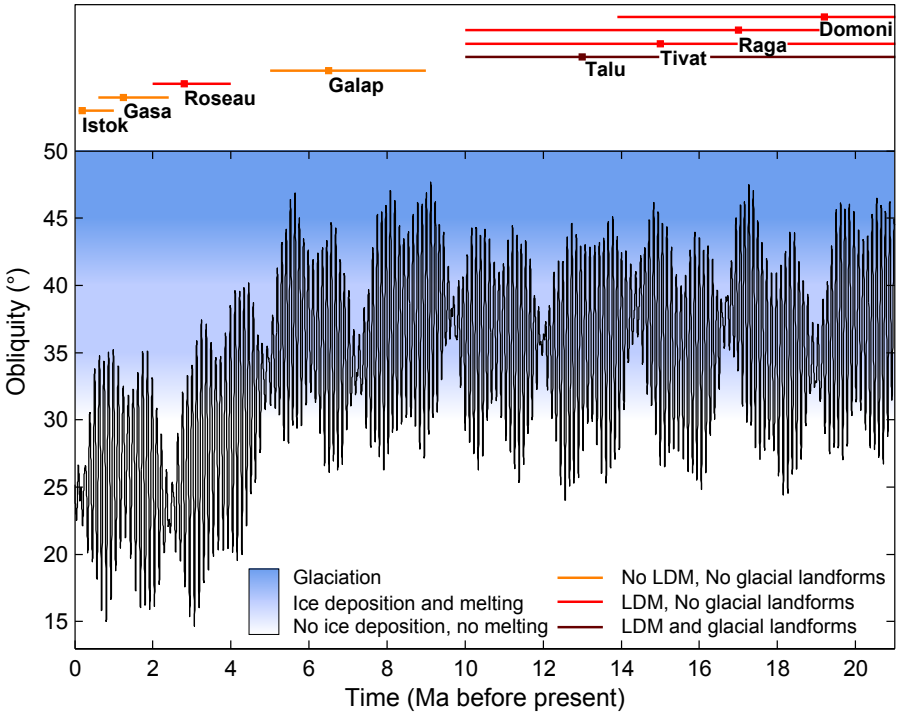

Figure 10. Martian obliquity in the last 21 My [*Laskar et al.*, 2004], obliquity thresholds for melting [*Head et al.*, 2003] and glaciation [*Baker et al.*, 2010], and study crater ages and ice-related morphology within these craters. Young craters (Istok, Gasa and Galap) have no evidence for LDM and glacial landforms and may have formed by melting of restricted amounts of snow/ice or CO_2 triggered flows. Older craters that have experienced substantial high-obliquity periods (>40-45°) are affected by LDM and/or glacial activity and may have undergone multiple gully accumulation-degradation cycles.

640 **Table 1.** Study crater characteristics.

Crater	Latitude	Longitude	Diameter (km)	Landform assemblage	Age	Age source
Istok	45.1°S	274.2°E	4.7	No LDM, No glacial landforms	0.19 (0.1–1.0) Ma	*Johnsson et al.* [2014]
Gasa	35.7°S	129.5°E	6.5	No LDM, No glacial landforms	1.25 (0.6–2.4) Ma	*Schon et al.* [2009]
Roseau	41.7°S	150.6°E	6.2	LDM, No glacial landforms	2.8 (2–4) Ma	Figure A.1
Galap	37.7°S	192.9°E	5.6	No LDM, No glacial landforms	6.5 (5–9) Ma	*De Haas et al.* [2015c]
Talu	40.3°S	20.1°E	9.1	LDM & glacial landforms	13 (10–22) Ma	Figure A.1
Tivat	45.9°S	9.5°E	3.1	LDM, No glacial landforms	15 (10–40) Ma	Figure A.1
Raga	48.1°S	242.4°E	3.4	LDM, No glacial landforms	17 (10–30) Ma	Figure A.1
Domoni	51.4°N	234.2°E	14	LDM, No glacial landforms	19.2 (13.9–24.5) Ma	*Viola et al.* [2015]
Flateyri	35.9°S	330.9°E	9.5	LDM & glacial landforms	51 (30–100) Ma	Figure A.1
Taltal	39.5°S	234.4°E	9.8	LDM & glacial landforms	220 (100–400) Ma	Figure A.1
Moni	47.0°S	18.8°E	5.0	LDM & glacial landforms	570 (400–900) Ma	Figure A.1
Artik	34.8°S	131.0°E	5.2	LDM & glacial landforms	590 (300–1000) Ma	Figure A.1
Hale	35.5°S	323.5°E	140	LDM & glacial landforms	$\sim$ 1 Ga	*Jones et al.* [2011]
Corozal	38.7°S	159.4°E	8.0	LDM & glacial landforms	1.4 (0.8–2.5) Ga	Figure A.1
Palikir	41.5°S	202.2°E	16	LDM & glacial landforms	1.8 (1.1–2.8) Ga	Figure A.1
Nqulu	37.9°S	169.6°E	20	LDM & glacial landforms	1.8 (1–3.5) Ga	Figure A.1
Langtang	38.1°S	224.0°E	9.2	LDM & glacial landforms	1.8 (1–3) Ga	Figure A.1
Lyot	50.5°N	29.4°E	115	LDM & glacial landforms	n.a. (1.6–3.3) Ga	*Dickson et al.* [2009]
Bunnik	37.8°S	217.9°E	28	LDM & glacial landforms	3.4 (3–3.7) Ga	Figure A.1

641 **Table 2.** List of data sources and vertical accuracy for the DTMs used to calculate alcove volumes. DTMs
642 from the University of Arizona were downloaded from the HiRISE website (http://www.uahirise.org/dtm/),
643 the other DTMs were made by the authors. DTM's with credit Open University or Birckbeck University of
644 London were made with SocetSet, DTM's with credit University of Texas were made with the Ames Stereo
645 Pipeline. Vertical precision was estimated via the method of *Kirk et al.* [2008].

Crater	HiRISE image 1	Pixel scale image 1 (m)	HiRISE image 2	Pixel scale image 2 (m)	Convergence angle (°)	Vertical precision (m)	DTM credit
Istok	PSP_006837_1345	0.250	PSP_007127_1345	0.258	20.1	0.14	Open University
Gasa (1)	ESP_021584_1440	0.255	ESP_022217_1440	0.279	20.8	0.15	University of Arizona
Gasa (2)	ESP_014081_1440	0.507	ESP_014147_1440	0.538	20.7	0.28	University of Arizona
Roseau	ESP_024115_1380	0.252	ESP_011509_1380	0.255	7.2	0.40	University of Texas
Galap	PSP_003939_1420	0.256	PSP_003939_1420	0.291	21.7	0.15	Open University
Talu	ESP_011672_1395	0.26	ESP_011817_1395	0.26	15.7	0.18	Open University
Tivat	ESP_012991_1335	0.25	ESP_013624_1335	0.26	17.3	0.17	University of Arizona
Raga	ESP_014011_1315	0.25	ESP_014288_1315	0.27	21.1	0.14	University of Arizona
Domoni (1)	ESP_016213_2315	0.30	ESP_016714_2315	0.31	18.1	0.19	University of Arizona
Domoni (2)	ESP_016846_2320	0.32	ESP_016569_2320	0.30	15.7	0.22	University of Arizona
Flateyri	ESP_022315_1440	0.257	ESP_030517_1440	0.258	0.8	3.7	University of Texas
Taltal	ESP_037074_1400	0.505	ESP_031259_1400	0.502	5.9	0.98	University of Texas
Moni	PSP_007110_1325	0.26	PSP_006820_1325	0.25	19.2	0.15	University of Arizona
Artik	ESP_012459_1450	0.27	ESP_012314_1450	0.25	14.5	0.21	University of Arizona
Hale (1)	ESP_012241_1440	0.26	ESP_012663_1440	0.26	15.3	0.19	University of Arizona
Hale (2)	ESP_030715_1440	0.29	ESP_030570_1440	0.26	15.7	0.20	University of Arizona
Hale (3)	PSP_002932_1445	0.26	PSP_003209_1445	0.27	24.9	0.12	Birkbeck University of London
Corozal	PSP_006261_1410	0.25	ESP_014093_1410	0.29	28.7	0.10	University of Arizona
Palikir	PSP_005943_1380	0.25	ESP_011428_1380	0.26	16.9	0.17	University of Arizona
Nqulu	PSP_004085_1420	0.27	PSP_004019_1420	0.25	20.4	0.14	Birkbeck University of London
Langtang	ESP_024099_1415	0.28	ESP_023809_1415	0.25	30.9	0.09	University of Arizona
Lyot	PSP_008823_2310	0.31	PSP_009245_2310	0.32	17.2	0.20	University of Arizona
Bunnik	PSP_002659_1420	0.26	PSP_002514_1420	0.25	13.6	0.21	University of Arizona

646 # A: Host crater dating

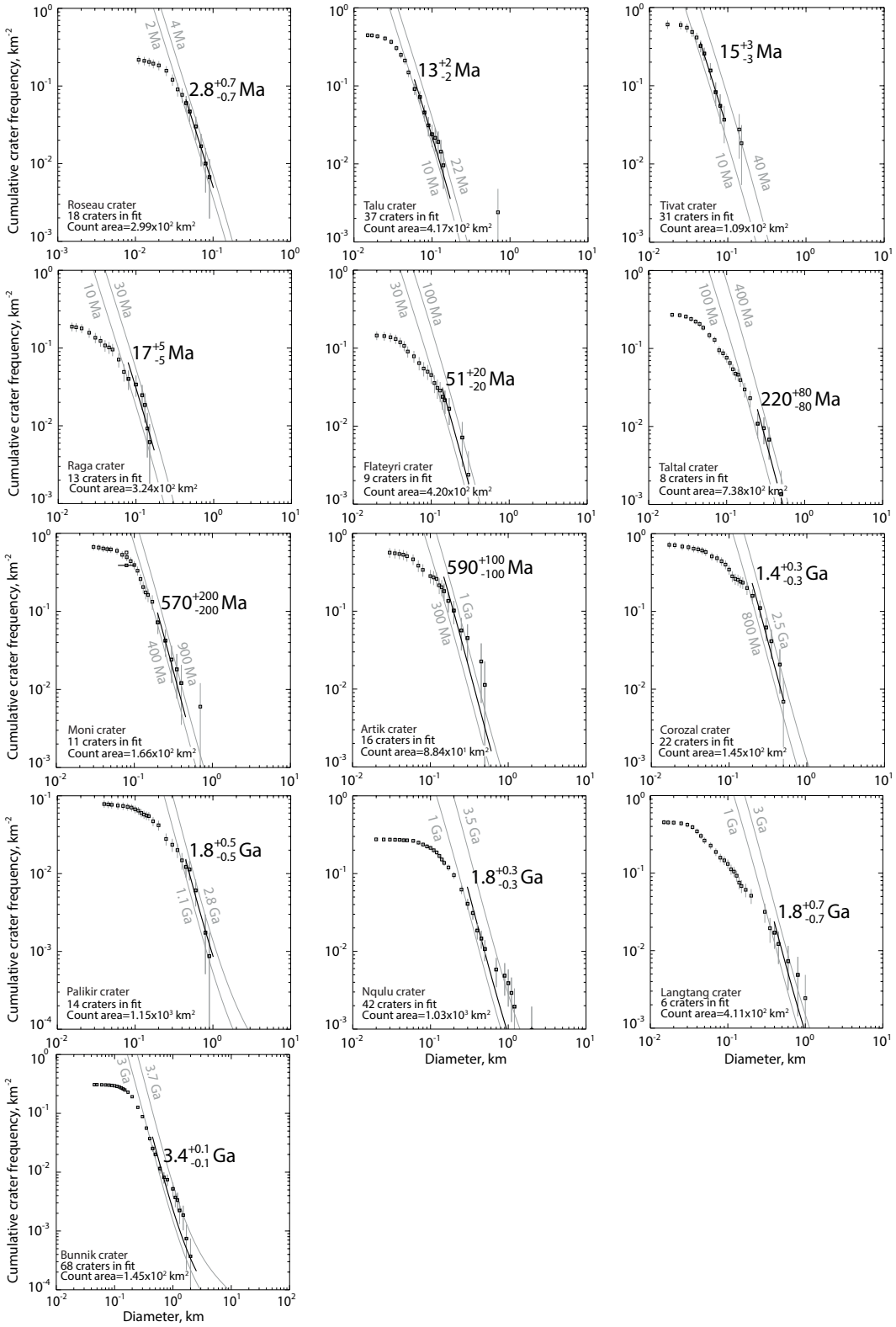

Figure A.1. Crater-size-frequency distributions of dated craters. Crater ages were defined based on the crater-size-frequency distribution using the chronology model of *Hartmann and Neukum* [2001] and the production function of *Ivanov* [2001]. Roseau crater: count performed on CTX image B05_011443_1380_XI_42S209W. Talu crater: count performed on CTX image B05_011672_1394_XN_40S339W. Tivat crater: count performed on CTX image B10_013624_1338_XN_46S350W. Raga crater: count performed on CTX image D10_031206_1316_XN_48S117W. Flateyri crater: count performed on CTX images P02_001745_1439_XN_36S029W and P15_007059_1438_XN_36S029W. Taltal crater: count per-

References

Arfstrom, J., and W. K. Hartmann (2005), Martian flow features, moraine-like ridges, and gullies: Terrestrial analogs and interrelationships, *Icarus*, *174*(2), 321–335.

Aston, A., S. Conway, and M. Balme (2011), Identifying Martian gully evolution, *Geological Society, London, Special Publications*, *356*(1), 151–169.

Baker, D. M., and J. W. Head (2015), Extensive Middle Amazonian mantling of debris aprons and plains in Deuteronilus Mensae, Mars: Implications for the record of mid-latitude glaciation, *Icarus*, *260*, 269–288.

Baker, D. M., J. W. Head, and D. R. Marchant (2010), Flow patterns of lobate debris aprons and lineated valley fill north of Ismeniae Fossae, Mars: Evidence for extensive mid-latitude glaciation in the Late Amazonian, *Icarus*, *207*(1), 186–209.

Ballantyne, C. K. (2002), Paraglacial geomorphology, *Quaternary Science Reviews*, *21*(18), 1935–2017.

Balme, M., N. Mangold, D. Baratoux, F. Costard, M. Gosselin, P. Masson, P. Pinet, and G. Neukum (2006), Orientation and distribution of recent gullies in the southern hemisphere of Mars: observations from High Resolution Stereo Camera/Mars Express (HRSC/MEX) and Mars Orbiter Camera/Mars Global Surveyor (MOC/MGS) data, *Journal of Geophysical Research: Planets (1991–2012)*, *111*(E5), E05,001.

Berman, D. C., W. K. Hartmann, D. A. Crown, and V. R. Baker (2005), The role of arcuate ridges and gullies in the degradation of craters in the Newton Basin region of Mars, *Icarus*, *178*(2), 465–486.

Berman, D. C., D. A. Crown, and L. F. Bleamaster (2009), Degradation of mid-latitude craters on Mars, *Icarus*, *200*(1), 77–95.

Berman, D. C., D. A. Crown, and E. C. Joseph (2015), Formation and mantling ages of lobate debris aprons on Mars: Insights from categorized crater counts, *Planetary and Space Science*, *111*, 83–99.

Beyer, R., O. Alexandrov, and Z. Moratto (2014), Aligning terrain model and laser altimeter point clouds with the Ames Stereo Pipeline, in *Lunar and Planetary Science Conference*, vol. 45, p. 2902.

Blair, T. C., and J. G. McPherson (2009), Processes and forms of alluvial fans, in *Geomorphology of Desert Environments*, edited by A. Parsons and A. Abrahams, pp. 413–467, Springer Netherlands.

Brough, S., B. Hubbard, and A. Hubbard (2016), Former extent of glacier-like forms on Mars, *Icarus*, *274*, 37–49.

Broxton, M. J., and L. J. Edwards (2008), The Ames Stereo Pipeline: Automated 3D surface reconstruction from orbital imagery, in *Lunar and Planetary Science Conference*, vol. 39, p. 2419.

Cedillo-Flores, Y., A. H. Treiman, J. Lasue, and S. M. Clifford (2011), CO_2 gas fluidization in the initiation and formation of Martian polar gullies, *Geophysical Research Letters*, *38*(21), L21,202.

Christensen, P. R. (2003), Formation of recent Martian gullies through melting of extensive water-rich snow deposits, *Nature*, *422*(6927), 45–48.

Christiansen, H. H. (1998), Nivation forms and processes in unconsolidated sediments, NE Greenland, *Earth Surface Processes and Landforms*, *23*(8), 751–760.

Church, M., and J. M. Ryder (1972), Paraglacial sedimentation: a consideration of fluvial processes conditioned by glaciation, *Geological Society of America Bulletin*, *83*(10), 3059–3072.

Conway, S. (This Issue), Gullies review, *Gullies special issue: Geological Society of London*.

Conway, S. J. (2010), Debris flows on earth and mars, Ph.D. thesis, Open University.

Conway, S. J., and M. Balme (2016), A novel topographic parameterization scheme indicates that martian gullies display the signature of liquid water, *Earth and Planetary Science Letters*, *454*, 36–45.

Conway, S. J., and M. R. Balme (2014), Decameter thick remnant glacial ice deposits on Mars, *Geophysical Research Letters*, *41*(15), 5402–5409.

Conway, S. J., M. R. Balme, J. B. Murray, M. C. Towner, C. H. Okubo, and P. M. Grindrod (2011), The indication of Martian gully formation processes by slope–area analysis, *Geological Society, London, Special Publications*, *356*(1), 171–201.

Conway, S. J., M. R. Balme, M. A. Kreslavsky, J. B. Murray, and M. C. Towner (2015), The comparison of topographic long profiles of gullies on Earth to gullies on Mars: a signal of water on Mars, *Icarus*, *253*, 189–204.

Costard, F., F. Forget, N. Mangold, and J. P. Peulvast (2002), Formation of Recent Martian Debris Flows by Melting of Near-Surface Ground Ice at High Obliquity, *Science*, *295*(5552), 110–113.

De Haas, T., E. Hauber, and M. G. Kleinhans (2013), Local late Amazonian boulder breakdown and denudation rate on Mars, *Geophysical Research Letters*, *40*, 3527–3531.

De Haas, T., E. Hauber, S. J. Conway, H. van Steijn, A. Johnsson, and M. G. Kleinhans (2015a), Earth-like aqueous debris-flow activity on Mars at high orbital obliquity in the last million years, *Nature Communications*, *6:7543*.

De Haas, T., D. Ventra, E. Hauber, S. J. Conway, and M. G. Kleinhans (2015b), Sedimentological analyses of Martian gullies: the subsurface as the key to the surface, *Icarus*, *258*, 92–108.

De Haas, T., S. J. Conway, and M. Krautblatter (2015c), Recent (Late Amazonian) enhanced backweathering rates on Mars: Paracratering evidence from gully alcoves, *Journal of Geophysical Research: Planets*, *120*(12), 2169–2189.

Dickson, J., C. Fassett, and J. Head (2009), Amazonian-aged fluvial valley systems in a climatic microenvironment on Mars: Melting of ice deposits on the interior of Lyot Crater, *Geophysical Research Letters*, *36*, L08,201.

Dickson, J. L., and J. W. Head (2009), The formation and evolution of youthful gullies on Mars: Gullies as the late-stage phase of Mars most recent ice age, *Icarus*, *204*(1), 63–86.

Dickson, J. L., J. W. Head, and M. Kreslavsky (2007), Martian gullies in the southern mid-latitudes of Mars: Evidence for climate-controlled formation of young fluvial features based upon local and global topography, *Icarus*, *188*(2), 315 – 323.

Dickson, J. L., J. W. Head, and D. R. Marchant (2008), Late Amazonian glaciation at the dichotomy boundary on Mars: Evidence for glacial thickness maxima and multiple glacial phases, *Geology*, *36*(5), 411–414.

Dickson, J. L., J. W. Head, T. A. Goudge, and L. Barbieri (2015), Recent climate cycles on Mars: Stratigraphic relationships between multiple generations of gullies and the latitude dependent mantle, *Icarus*, *252*, 83–94.

Dundas, C. M., A. S. McEwen, S. Diniega, S. Byrne, and S. Martinez-Alonso (2010), New and recent gully activity on Mars as seen by HiRISE, *Geophysical Research Letters*, *37*(7), L07,202.

Dundas, C. M., S. Diniega, C. J. Hansen, S. Byrne, and A. S. McEwen (2012), Seasonal activity and morphological changes in Martian gullies, *Icarus*, *220*(1), 124–143.

Dundas, C. M., S. Diniega, and A. S. McEwen (2015), Long-Term Monitoring of Martian Gully Formation and Evolution with MRO/HiRISE, *Icarus*, *251*, 244–263.

763 Fassett, C. I., J. S. Levy, J. L. Dickson, and J. W. Head (2014), An extended period of
764 episodic northern mid-latitude glaciation on Mars during the Middle to Late Amazo-
765 nian: Implications for long-term obliquity history, *Geology*, *42*(9), 763–766.
766 Forget, F., R. M. Haberle, F. Montmessin, B. Levrard, and J. W. Head (2006), Formation
767 of glaciers on mars by atmospheric precipitation at high obliquity, *Science*, *311*(5759),
768 368–371.
769 Harrison, T. N., G. R. Osinski, L. L. Tornabene, and E. Jones (2015), Global documenta-
770 tion of gullies with the Mars Reconnaissance Orbiter Context Camera and implications
771 for their formation, *Icarus*, *252*, 236–254.
772 Hartmann, W. K., and G. Neukum (2001), Cratering chronology and the evolution of
773 Mars, in *Chronology and evolution of Mars*, pp. 165–194, Springer.
774 Hartmann, W. K., V. Ansan, D. C. Berman, N. Mangold, and F. Forget (2014), Compre-
775 hensive analysis of glaciated martian crater Greg, *Icarus*, *228*, 96–120.
776 Head, J. W., J. F. Mustard, M. A. Kreslavsky, R. E. Milliken, and D. R. Marchant (2003),
777 Recent ice ages on Mars, *Nature*, *426*, 797–802.
778 Head, J. W., D. R. Marchant, and M. A. Kreslavsky (2008), Formation of gullies on Mars:
779 Link to recent climate history and insolation microenvironments implicate surface water
780 flow origin, *Proceedings of the National Academy of Sciences*, *105*(36), 13,258–13,263.
781 Head, J. W., D. R. Marchant, J. L. Dickson, A. M. Kress, and D. M. Baker (2010), North-
782 ern mid-latitude glaciation in the Late Amazonian period of Mars: Criteria for the
783 recognition of debris-covered glacier and valley glacier landsystem deposits, *Earth and*
784 *Planetary Science Letters*, *294*(3), 306–320.
785 Heldmann, J. L., and M. T. Mellon (2004), Observations of Martian gullies and con-
786 straints on potential formation mechanisms, *Icarus*, *168*(2), 285 – 304.
787 Heldmann, J. L., O. B. Toon, W. H. Pollard, M. T. Mellon, J. Pitlick, C. P. McKay, and
788 D. T. Andersen (2005), Formation of Martian gullies by the action of liquid water
789 flowing under current Martian environmental conditions, *J. Geophys. Res.*, *110*(E5),
790 E05,004.
791 Hubbard, B., R. E. Milliken, J. S. Kargel, A. Limaye, and C. Souness (2011), Geomor-
792 phological characterisation and interpretation of a mid-latitude glacier-like form: Hellas
793 Planitia, Mars, *Icarus*, *211*(1), 330–346.
794 Ivanov, B. A. (2001), Mars/Moon cratering rate ratio estimates, in *Chronology and evolu-*
795 *tion of Mars*, pp. 87–104, Springer.

Johnsson, A., D. Reiss, E. Hauber, H. Hiesinger, and M. Zanetti (2014), Evidence for very recent melt-water and debris flow activity in gullies in a young mid-latitude crater on Mars, *Icarus*, *235*, 37–54.

Jones, A., A. McEwen, L. Tornabene, V. Baker, H. Melosh, and D. Berman (2011), A geomorphic analysis of Hale crater, Mars: The effects of impact into ice-rich crust, *Icarus*, *211*(1), 259–272.

Kirk, R., E. Howington-Kraus, M. Rosiek, J. Anderson, B. Archinal, K. Becker, D. Cook, D. Galuszka, P. Geissler, T. Hare, et al. (2008), Ultrahigh resolution topographic mapping of Mars with MRO HiRISE stereo images: Meter-scale slopes of candidate Phoenix landing sites, *Journal of Geophysical Research: Planets (1991–2012)*, *113*(E3), E00A24.

Kneissl, T., D. Reiss, S. Van Gasselt, and G. Neukum (2010), Distribution and orientation of northern-hemisphere gullies on Mars from the evaluation of HRSC and MOC-NA data, *Earth and Planetary Science Letters*, *294*(3), 357–367.

Kneissl, T., S. van Gasselt, and G. Neukum (2011), Map-projection-independent crater size-frequency determination in GIS environments - New software tool for ArcGIS, *Planetary and Space Science*, *59*(11), 1243–1254.

Kreslavsky, M., and J. Head (2002), Mars: Nature and evolution of young latitude-dependent water-ice-rich mantle, *Geophysical Research Letters*, *29*(15), doi: 10.1029/2002GL015392.

Kreslavsky, M. A., J. W. Head, and D. R. Marchant (2008), Periods of active permafrost layer formation during the geological history of Mars: Implications for circum-polar and mid-latitude surface processes, *Planetary and Space Science*, *56*(2), 289–302.

Kumar, P. S., J. W. Head, and D. A. Kring (2010), Erosional modification and gully formation at Meteor Crater, Arizona: Insights into crater degradation processes on Mars, *Icarus*, *208*(2), 608–620.

Laskar, J., A. Correia, M. Gastineau, F. Joutel, B. Levrard, and P. Robutel (2004), Long term evolution and chaotic diffusion of the insolation quantities of mars, *Icarus*, *170*(2), 343 – 364.

Levrard, B., F. Forget, F. Montmessin, and J. Laskar (2007), Recent formation and evolution of northern Martian polar layered deposits as inferred from a Global Climate Model, *Journal of Geophysical Research: Planets*, *112*(E6), E06,012.

Levy, J., J. Head, D. Marchant, J. Dickson, and G. Morgan (2009), Geologically recent gully–polygon relationships on Mars: Insights from the Antarctic Dry Valleys on the roles of permafrost, microclimates, and water sources for surface flow, *Icarus*, *201*(1), 113–126.

Levy, J., J. Head, J. Dickson, C. Fassett, G. Morgan, and S. Schon (2010a), Identification of gully debris flow deposits in Protonilus Mensae, Mars: Characterization of a water-bearing, energetic gully-forming process, *Earth and Planetary Science Letters*, *294*(34), 368–377.

Levy, J., J. W. Head, and D. R. Marchant (2010b), Concentric crater fill in the northern mid-latitudes of Mars: Formation processes and relationships to similar landforms of glacial origin, *Icarus*, *209*(2), 390–404.

Madeleine, J.-B., F. Forget, J. W. Head, B. Levrard, F. Montmessin, and E. Millour (2009), Amazonian northern mid-latitude glaciation on Mars: A proposed climate scenario, *Icarus*, *203*(2), 390–405.

Madeleine, J.-B., J. Head, F. Forget, T. Navarro, E. Millour, A. Spiga, A. Colaïtis, A. Määttänen, F. Montmessin, and J. Dickson (2014), Recent Ice Ages on Mars: The role of radiatively active clouds and cloud microphysics, *Geophysical Research Letters*, *41*(14), 4873–4879.

Malin, M. C., and K. S. Edgett (2000), Evidence for Recent Groundwater Seepage and Surface Runoff on Mars, *Science*, *288*(5475), 2330–2335.

McEwen, A. S., E. M. Eliason, J. W. Bergstrom, N. T. Bridges, C. J. Hansen, W. A. Delamere, J. A. Grant, V. C. Gulick, K. E. Herkenhoff, L. Keszthelyi, et al. (2007), Mars reconnaissance orbiter's high resolution imaging science experiment (HiRISE), *Journal of Geophysical Research: Planets*, *112*(E5), E05S02.

Michael, G. G., and G. Neukum (2010), Planetary surface dating from crater size–frequency distribution measurements: Partial resurfacing events and statistical age uncertainty, *Earth and Planetary Science Letters*, *294*(3), 223–229.

Milliken, R., J. Mustard, and D. Goldsby (2003), Viscous flow features on the surface of Mars: Observations from high-resolution Mars Orbiter Camera (MOC) images, *Journal of Geophysical Research: Planets (1991–2012)*, *108*(E6), 5057.

Mustard, J. F., C. D. Cooper, and M. K. Rifkin (2001), Evidence for recent climate change on Mars from the identification of youthful near-surface ground ice, *Nature*, *412*(6845), 411–414.

Núñez, J., O. Barnouin, S. Murchie, F. Seelos, J. McGovern, K. Seelos, and D. Buczkowski (2016), New insights into gully formation on Mars: Constraints from composition as seen by MRO/CRISM, *Geophysical Research Letters*, doi: 10.1002/2016GL068956.

Okubo, C. H., L. L. Tornabene, and N. L. Lanza (2011), Constraints on mechanisms for the growth of gully alcoves in Gasa crater, Mars, from two-dimensional stability assessments of rock slopes, *Icarus*, *211*(1), 207–221.

Pelletier, J. D., K. J. Kolb, A. S. McEwen, and R. L. Kirk (2008), Recent bright gully deposits on Mars: Wet or dry flow?, *Geology*, *36*(3), 211–214.

Pickett, S. T. (1989), Space-for-time substitution as an alternative to long-term studies, in *Long-term studies in ecology*, pp. 110–135, Springer.

Pilorget, C., and F. Forget (2016), Formation of gullies on mars by debris flows triggered by co2 sublimation, *Nature Geoscience*, *9*(1), 65–69.

Raack, J., D. Reiss, and H. Hiesinger (2012), Gullies and their relationships to the dust–ice mantle in the northwestern Argyre Basin, Mars, *Icarus*, *219*(1), 129–141.

Reiss, D., S. van Gasselt, G. Neukum, and R. Jaumann (2004), Absolute dune ages and implications for the time of formation of gullies in Nirgal Vallis, Mars, *Journal of Geophysical Research: Planets*, *109*(E6), E06,007.

Reiss, D., E. Hauber, H. Hiesinger, R. Jaumann, F. Trauthan, F. Preusker, M. Zanetti, M. Ulrich, A. Johnsson, L. Johansson, et al. (2011), Terrestrial gullies and debris-flow tracks on Svalbard as planetary analogs for Mars, *Geological Society of America Special Papers*, *483*, 165–175.

Schon, S. C., and J. W. Head (2011), Keys to gully formation processes on Mars: Relation to climate cycles and sources of meltwater, *Icarus*, *213*(1), 428 – 432.

Schon, S. C., and J. W. Head (2012), Gasa impact crater, Mars: Very young gullies formed from impact into latitude-dependent mantle and debris-covered glacier deposits?, *Icarus*, *218*(1), 459–477.

Schon, S. C., J. W. Head, and C. I. Fassett (2009), Unique chronostratigraphic marker in depositional fan stratigraphy on Mars: Evidence for ca. 1.25 Ma gully activity and surficial meltwater origin, *Geology*, *37*, 207–210.

Schon, S. C., J. W. Head, and C. I. Fassett (2012), Recent high-latitude resurfacing by a climate-related latitude-dependent mantle: Constraining age of emplacement from counts of small craters, *Planetary and Space Science*, *69*(1), 49–61.

Shean, D. E., O. Alexandrov, Z. M. Moratto, B. E. Smith, I. R. Joughin, C. Porter, and P. Morin (2016), An automated, open-source pipeline for mass production of digital elevation models (DEMs) from very-high-resolution commercial stereo satellite imagery, *ISPRS Journal of Photogrammetry and Remote Sensing*, *116*, 101–117.

Smith, I. B., N. E. Putzig, J. W. Holt, and R. J. Phillips (2016), An ice age recorded in the polar deposits of Mars, *Science*, *352*(6289), 1075–1078.

Souness, C., B. Hubbard, R. E. Milliken, and D. Quincey (2012), An inventory and population-scale analysis of martian glacier-like forms, *Icarus*, *217*(1), 243–255.

Squyres, S. W. (1979), The distribution of lobate debris aprons and similar flows on Mars, *Journal of Geophysical Research: Solid Earth*, *84*(B14), 8087–8096.

Treiman, A. H. (2003), Geologic settings of Martian gullies: Implications for their origins, *Journal of Geophysical Research: Planets (1991–2012)*, *108*(E4).

Vincendon, M. (2015), Identification of mars gully activity types associated with ice composition, *Journal of Geophysical Research: Planets*, *120*(11), 1859–1879.

Viola, D., A. S. McEwen, C. M. Dundas, and S. Byrne (2015), Expanded secondary craters in the Arcadia Planitia region, Mars: Evidence for tens of Myr-old shallow subsurface ice, *Icarus*, *248*, 190–204.

Williams, K., O. Toon, J. Heldmann, and M. Mellon (2009), Ancient melting of mid-latitude snowpacks on Mars as a water source for gullies, *Icarus*, *200*(2), 418 – 425.